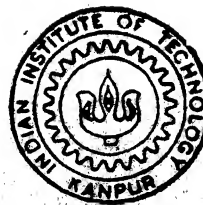


7210101

# LDA MEASUREMENTS IN CO-AXIAL JET FLOWS WITH IMPOSED PRESSURE GRADIENT

by

AMIT GOYAL



Th.  
AE/1994/M  
G 7482

AE  
1994  
M  
GOY  
LDA

DEPARTMENT OF AEROSPACE ENGINEERING  
INDIAN INSTITUTE OF TECHNOLOGY KANPUR

April, 1994

# LDA MEASUREMENTS IN CO-AXIAL JET FLOWS WITH IMPOSED PRESSURE GRADIENT

A Thesis submitted  
In Partial Fulfilment of The Requirements  
for the Degree of

MASTER OF TECHNOLOGY

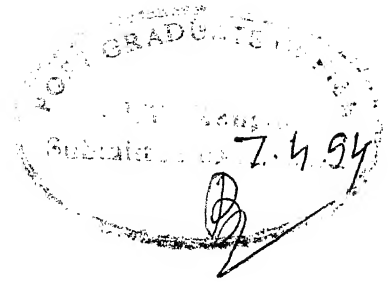
*By*

AMIT GOYAL

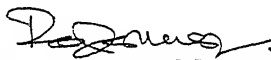
Department of Aerospace Engineering  
INDIAN INSTITUTE OF TECHNOLOGY, KANPUR

APRIL, 1994

CERTIFICATE



This is to certify that the thesis entitled "LDA Measurements In Co-Axial Jet Flows With Imposed Pressure Gradient" is a record of work under my supervision and that it has not been submitted elsewhere for awarding degree.

 7.4.94  
Dr. R.K. Sullerey

Department of Aerospace Engineering  
Indian Institute Of Technology  
Kanpur Pin - 208 016

## ACKNOWLEDGEMENTS

I express my heartfelt gratitude to my guide Dr. R.K.Sullerey, department of Aerospace Engineering, IIT Kanpur. I owe a special debt for his invaluable guidance and encouragement given to me at each and every stage of my project, without which this study would not have been successfully completed.

I wish to thank Mr. A.K.Rajpal for his assistance in initiating the experimental analysis.

I wish to acknowledge the assistance given to me by Mr.V.C.Srivastava in experimental set-up. Thanks is also due to Mr. J.B.Mishra for his help in experimental set-up.

I wish to express my thanks to Mr Chauhan for his cooperation in providing air supply.

I also wish to thank Mr. Bhattacharya, In charge of Aerospace Engineering Workshop for providing cooperation in manufacturing work.

Last but not the least, I would like to thank my friends for their invaluable help at various stages of this project.

KANPUR

DATED

AMIT GOYAL

## Contents

	Page
Abstract.....	v
List of symbols.....	vi
List of figures.....	vii
Introduction.....	1
Review of literature.....	5
Scope of present work.....	11
Experimental set-up.....	13
Results and discussion.....	17
Conclusions.....	24
Bibliography.....	25
Figures.....	28

### Abstract

The present investigations report LDA measurements in co-axial jet flows with imposed pressure gradient. A four degree semi-divergence angle is provided in the upper and lower walls of the test section. This does not allow flow separation, however, an adverse pressure gradient is imposed in the streamwise direction. Comparison has been made with the results of flow without pressure gradient, for identical flow conditions. The experiments are conducted at two different values of free stream turbulence and velocity ratios ranging from 0.10 to 0.33. It is seen that the presence of an imposed pressure gradient results in a more rapid decrease in the centreline velocity. The jet half radius increases in adverse pressure gradient. The peak value of turbulence intensity decreases at a given axial location. However, the location of the peak value shifts radially away from the axis. Similarity in the mean velocity profiles is observed for both constant area mixing and variable area mixing.

## List Of Symbols

$d$	:Nozzle exit diameter
$e_i$	:Unit vector in the direction of incident light
$e_s$	:Unit vector in the direction of scattered light
$f_i$	:Frequency of incident light
$f_s$	:Frequency of scattered light
FS TURB	:Free stream turbulence
FST	:Free stream turbulence
LDA	:Laser Doppler Anemometer
$R_o$	:Nozzle exit radius
$R_{1/2}$	:Radius where $U = 0.5(U_c - U_f)$
$U$	:Mean velocity in the axial direction
$U_c$	:Average centreline velocity
$U_f$	:Free stream velocity
$U_o$	:Jet exit velocity
$U_{rms}$	:Root mean square velocity in axial direction
VR	:Velocity ratio
VER	:Plane of Divergence
WPG	:with imposed pressure gradient
$x$	:Axial distance downstream from the nozzle exit
$\lambda$	:Wavelength of the incident light
$\theta$	:Angle of the beams intersection

## List Of Figures

Fig. No.	Page No.
1. Flow geometry.....	28
2. Tunnel layout.....	29
3. Nozzle.....	30
4. Axial distribution of centreline velocity.....	31
5. Axial distribution of centreline velocity.....	32
6. Axial distribution of centreline velocity.....	33
7. Axial distribution of centreline velocity.....	34
8. Distribution of streamwise turbulence on the axis.....	35
9. Distribution of streamwise turbulence on the axis.....	36
10. Distribution of streamwise turbulence on the axis.....	37
11. Distribution of streamwise turbulence on the axis.....	38
12. Variation of velocity defect along the axis.....	39
13. Variation of velocity defect along the axis.....	40
14. Variation of velocity defect along the axis.....	41
15. Variation of velocity defect along the axis.....	42
16. Axial distribution of jet half-radius.....	43
17. Axial distribution of jet half-radius.....	44
18. Axial distribution of jet half radius.....	45
19. Mean velocity profiles across the flow.....	46
20. Mean velocity profiles across the flow.....	47
21. Mean velocity profiles across the flow.....	48
22. Streamwise turbulence intensity across the flow.....	49
23. Streamwise turbulence intensity across the flow.....	50
24. Streamwise turbulence intensity across the flow.....	51
25. Streamwise turbulence intensity across the flow.....	52



25.	Streamwise turbulence intensity across the flow.....	52
26.	Streamwise turbulence intensity across the flow.....	53
27.	Variation of U-intensity across the flow.....	54
28.	Variation of U-intensity across the flow.....	55
29.	Variation of U-intensity across the flow.....	56
30.	Similarity velocity profiles across the flow.....	57
31.	Similarity velocity profiles across the flow.....	58
32.	Similarity velocity profiles across the flow.....	59
33.	Similarity velocity profiles across the flow.....	60
34.	Similarity velocity profiles across the flow.....	61

## Introduction

Most of the flow phenomena of importance to engineers involve turbulence; there is therefore a great need for designers to be able to predict the behaviour of turbulent flows. In a wide variety of engineering flow situations, we encounter the process of turbulent mixing of two fluid streams. Some such applications include fuel injection in turbojet, ramjet and piston engines, processing in chemical and food production and dispersion of pollutants in water ways and the atmosphere.

Co-axially flowing gaseous streams have attracted the attention of various investigators, as it finds several physical applications such as in jet engine combustion chambers, thrust augmentation devices, ejectors and in design of any device involving mixing of different streams.

Co-flowing jets expanding in ducts are known as confined jets. Confined jets generally produce an axial pressure gradient which is intimately coupled to the mixing process, and vice versa. The confined jet study is also important in understanding the basic flow phenomena of mixing. For example, it involves boundary layer flows in adverse pressure gradients, regions of similar velocity profiles, boundary layer separation, reattachment etc.

The present work is an experimental investigation of confined air jet with a co-flowing secondary air stream. The experiment is conducted at different velocity ratios ( ratio of free stream velocity to the jet velocity ) with different free stream turbulence. This work differs from previous studies as effect of imposed pressure gradient is also studied. Most of the

measurements are conducted using LDA technique. The mixing process is turbulent in nature and the measurement technique in turbulent flows plays an important role.

LDA is a unique tool for fluid flow measurements. It is characterised by its outstanding features in fluid flow measurements which ensure a high degree of accuracy and excellent performance. In LDA measurements, even though the fluid velocity is of primary interest, the LDA signal originates from the tracer particles called seeding, present in the fluid and LDA actually measures the velocity of the seeding particles. Thus it is important that sufficient number of particles be present in the fluid and they scatter sufficient light to produce LDA signal. Secondly, the tracer particles should follow the fluid with high fidelity. Size of the particles is also of considerable importance. If all the requirements are met it provides excellent results. LDA technique has obvious advantages over other techniques of velocity measurements.

- (i) Non-contact probing system which does not disturb the flow.
- (ii) It has excellent spatial-resolution characteristics which determine the instantaneous velocity of a fluid element.
- (iii) It has calibration-free output voltages which have linear relation with flow-velocity.
- (iv) The optical method used for the fluid flow measurement offers substantial advantages over alternative methods in a particular flow situation. This also permits the measurements of local, instantaneous velocity of tracer particles suspended in the flow without disturbing the flow field.

- (v) Non-disturbing flow measuring technique provides a significant tool specially relevant to recirculating flows.
- (vi) The hot wire and hot film anemometer, the principal experimental tools for quantitative investigations of the structure of turbulent flows are limited to applications in:
  - (a) Low temperature
  - (b) Low speed
  - (c) Low turbulent intensity flows, and
  - (d) Flow outside regions of recirculation.
 Most of these shortcomings are overcome by LDA, although it has its own limitations.
- (vii) By appropriate choice of the laser and the signal processing equipment, LDA is applicable for measurements in flows of liquids and gases in ducts, particularly for toxic, corrosive fluid flows.

#### Principle :

LDA utilizes laser beam for velocity probing and is based on the "Doppler-shift effect". The apparent change in the frequency of wave motion due to relative motion of the source and receiver, is known as the "Doppler-shift". When the beam passes through the fluid flow, light is scattered by the particles suspended in the fluid. The scattered light reveals the information about the velocity which is interpreted by opto-electronic means.

#### Doppler-shift effect :

The frequency relationship between a scattered light wave and incident light wave can be given by the vector equation :

$$f_s = f_i + (1/\lambda) v (e_s - e_i)$$

where,  $v$  = velocity of the particle

$f_s$  = frequency of scattered light

$f_i$  = frequency of incident light

$\lambda$  = wavelength of incident light

$e_i$  = unit vector in the direction of incident light wave

$e_s$  = unit vector in the direction of scattered light wave.

Hence  $f_s - f_i = (1/\lambda) v (e_s - e_i)$

Now  $f_s - f_i = f_D = \text{frequency shift}$

= Doppler frequency

Therefore  $f_D = (1/\lambda) v (e_s - e_i)$

Thus it is quite evident that the Doppler frequency is directly proportional to the particle velocity.

For all the modes of operation, the velocity component  $v$ , measured is one normal to the bisector of the beam intersection angle  $\theta$ , and parallel to the beam plane. Flow velocity is thus calculated from the formula:

$$v = \frac{f_D \times \lambda}{2 \sin (\theta/2)}$$

where  $\theta$  is the angle of beam intersection.

## Review of literature

Confined jet mixing with a thin inlet boundary layer condition exhibits a characteristic of free-jet mixing, boundary layer flow and potential core entrainment. For the general case of incompressible flow in co-flowing air streams, the flow field can be subdivided into three distinct regions with different characteristics.

Region 1 : The initial region consists that portion of the flow in which the central ( primary ) stream and the outer ( secondary ) stream include distinct potential cores. In addition, a wall boundary layer exists, as does a shear layer region between the two cores.

Region 2 : This is the transition region characterised by the absence of a potential core and by turbulent mixing across the entire duct cross section. The jet velocity and the shear stress distribution may be considered approximately self preserving.

Region 3 : In this region, the boundary layer gets merged with the jet. Thus no portion of the velocity profile is uniform in this region. The velocity profile continues to change until flow becomes fully developed. This region is generally much longer than the either two.

Fig. 1 illustrates the behaviour of a jet in axisymmetric duct of uniform/diverging cross section. Jet issuing from the nozzle of diameter (  $d$  ) with a uniform velocity (  $U_o$  ), is generally known as primary stream. The surrounding fluid with uniform velocity (  $U_f$  ) at the exit plane of the nozzle is known as secondary stream.

Landis and Shapiro (1) studied the turbulent spread of jet into a secondary flow. They found that in developed flow regions, the fully normalised profile shapes of velocity, temperature and concentration profiles are substantially alike and may be represented by a cosine profile. They concluded that the velocity ratio is the primary variable governing the mixing.

Curtet (2) developed approximate theory of confined jets. Experimental work was also presented. Two different test rigs were used to study various regimes of jets, effect of nozzle height and for the analysis of velocity and pressure distribution. Velocity was obtained by total and static pressure measurements. They showed that two distinct regimes can be identified, one in which the jet is accompanied by a recirculation eddy, and the other in which no eddy is formed.

Curtet and Ricou (3) made measurements in an axisymmetric ducted air jet of fluctuating mean velocities, jet width, secondary stream velocities, duct wall static pressure and the boundary layer thickness. Results were compared with the approximate jet theory. Pitot and hot wire measurements were made. They took special precaution to reduce initial turbulence level of ambient air stream as it effects the mixing process. Test conditions varied for different velocity ratios ranging from 0.09 to 0.5. They showed from experimental studies that the mean velocities tend to equilibrium profile but not the velocity fluctuations.

Bradbury and Riley (4) Carried out experimental investigations on co-flowing jets. On the basis of simple dimensional arguments, they showed that the results for the spread

of jets with different velocity ratios can be collapsed into a single universal curve provided the effective origins of the various sets of data can be shifted.

Durst and Whitelaw (5) made measurements of mean and fluctuating axial velocity components along the central line of a round tube and across the axis. These measurements were carried out using DISA frequency tracking demodulator and did not extend beyond seven diameters downstream of jet exit. Reference (6) presents the experimental data of the turbulent mixing of axi-symmetric gaseous streams. It presents three sets of data at different velocity ratios. Mean axial component of velocity and static temperature measurements were calculated in axial and radial direction.

Antonia and Bilger (7) made an experimental investigation of the flow development of axisymmetric jet exhausting into a moving air stream for two values of velocity ratios i.e. 0.22 and 0.33. The free stream turbulence level was 0.1 %. They concluded that the self preservation does not apply for turbulent structure at the flow far down stream and depends strongly on the complete past history.

Ramaprian and Chandrasekhar (8) conducted measurements on the mean and the most of the significant turbulent properties of plane isothermal and heated jets. The velocity measurements were made using two component, frequency-shifted Laser Doppler Anemometer. The LDA measurements indicated lower turbulence intensities and lower turbulent fluxes compared to the hot wire data.

Antonia and Bilger (9) presented analysis for predicting the development of an axisymmetric turbulent jet issuing into a co-flowing external air stream. They used a two-parameter model of



turbulence developed by Rodi and Spalding (10), which uses two differential equations for the turbulent energy and the length scale of the turbulence respectively. This model gave results similar to the experimental results at velocity ratio 0.33. This emphasised the non-similar character of the turbulence.

Smith and Hughes (11) made measurements in a turbulence circular jet in the presence of a co-flowing free stream using hot wire measurements. They concluded that the presence of free stream reduces the rate of decay of longitudinal turbulent component of the velocity. The mean velocity profiles were "bell shaped" form and became more similar as  $x/d$  was increased. Rate of spread of jet decreases as the velocity ratio increases.

Habib and Whitelaw (12) studied the velocity characteristics of confined co-axial jets with and without swirl. They measured through a combination of pressure probes, hot wire and LDA at velocity ratios 1 and 0.33. The results were compared with calculations, based on the solution of finite-difference forms of steady, Navier-Stokes equations, and an effective-viscosity hypothesis. They compared the results within the corner recirculation region with three types of instrumentation and showed that the serious errors of interpretation of mean velocity measurements need not arise. The two equation model was able to represent non-swirling flow and was less appropriate to the swirling flow. Choi et. al (14) studied the mixing of a subsonic confined air jet with a coaxial secondary air stream with an imposed adverse pressure gradient. The experimental study indicated that the presence of an adverse pressure gradient promotes more rapid mixing and spreading of shear layer in the

initial mixing region, as well as elevated turbulent normal stress and shear stress levels in the outer portions of the mixing layer after the primary and secondary streams have merged. Significant radial static pressure variations occur in both the initial mixing and the transition regions.

Singh et. al (16) studied the effect of imposed swirl on co-axial jets exhausting into confined space. They showed that the swirl in the central jet leads to faster mixing whereas higher swirl in the annular jet improves both mixing and development.

Sullerey (17) carried out LDA measurements in co-axial jet flows. He conducted experimental work on nozzle of diameter 1.8mm. Grids were used to produce different level of free stream turbulence. Comparison of LDA values and pitot tube values for mean velocity measurements, and LDA values and hot wire values for turbulence measurements was also shown.

So and Aksoy (18) investigated the self-preserving turbulent flows in the arbitrary stream. Incompressible and compressible gas jet in an arbitrary stream are analysed. The governing equations for incompressible and variable density jets and compressible density jets are identical, thus, the analysis of both cases is similar except for the case of perfect gas equation.

Kuhlman and Gross (19) used a three component LDA to acquire three-dimensional mean and fluctuating velocity measurements in a low-speed air jet entering a stagnant ambient, over the  $x/d$  range of 16. They showed that the mean velocity and Reynolds stress data approach a self-preserving behaviour beyond  $x/d$  value of 19.

However, the root mean square turbulence fluctuations were not found self preserving at the axial locations.

Johnson (20) studied the accuracy of well known turbulent models in simulating the mean velocity, turbulence and concentration fields for the cases of constant and variable density, turbulent, low Mach number, isothermal and co-axial streams. The standard  $k \sim \epsilon$  eddy viscosity model and an anisotropic thin shear algebraic stress model (ASM) were employed for constant density case.

## SCOPE OF THE PRESENT WORK

Mixing of subsonic confined air jets with a co-axial secondary stream has various applications. In most of its applications, the flow region adjacent to the jet exit is most important. The turbulent mixing in this region determines the chemical processes as in the mixing region of a hydrogen jet in a co-flowing air stream.

The aerodynamic conditions at the jet exit has been studied by various investigators. However, Choi et. al (14) have studied this under the effect of an imposed adverse pressure gradient using hot wire anemometer. Earlier, LDA measurements in confined jets were carried out with varying outer stream turbulence by Sullerey and Chalwade (13). In this work a frequency tracker was used instead of a counter processor. The investigations were limited to the regions of low mean velocity and turbulence levels due to the limitations of the setup. Investigations were also carried on co-flowing streams, using Laser Doppler Anemometer on a constant area test section by Sullerey (17).

In the present work, the velocity ratios ranging from 0.1 to 0.33 were used on two different values of free stream turbulence. This was achieved using specially designed wire grid. In the first stage of investigation, axial velocity and turbulence were measured for velocity ratios 0.11 to 0.33. Velocity and turbulence were also measured along the radial direction at  $x/d$  locations ranging from 10 to 50. No grid was used for this set of experiments.

In the second stage of investigation, axial velocity and turbulence were measured for velocity ratios from 0.1 to 0.33. Velocity and turbulence were also measured along the radial direction at  $x/d$  locations ranging from 10 to 60. A grid was used for this set of experiments. The average value of free stream turbulence were not identical although same grid was used for all the velocity ratios. The value of free stream turbulence varied from 1.15 % to 1.3 % when no grid is used and from 9.5 % to 10.8 % when grid is used.

The instrumentation was adjusted for maximum validation number. The semi-divergence angle of 4 degrees was chosen to generate an adverse pressure gradient and avoid flow separation. This type of situation may be encountered in the combustion chamber. The flow in the test section is considered to be symmetric. However, this is not perfectly correct because of the 4 degree semi-divergence angle on upper and lower walls of the test section. A set of data is also taken in the vertical direction with the help of pitot tube. A comparison has been made with the results of uniform area mixing, without any imposed pressure gradient.

### EXPERIMENTAL SET-UP

The experimental setup used for the present investigations is a basic facility for LDA measurements suitable for both cold and hot flows. The test section is made up of perspex sheet 10 mm thick. The cross section of the test section at the nozzle exit was 70 mm x 70 mm. The length of the test section was 445 mm. Upper and lower walls of the test section had a 4 degree angle of divergence, while the side walls were perfectly parallel. The side walls had laser quality quartz glass windows of thickness 6 mm and a size of 150 mm x 60 mm. Laser beams could pass through these windows and enable measurements upto  $x/d$  of 65. A 170 mm slot is provided on the top surface for pitot tube measurements. There is a provision to cover the slot while conducting experiment using LDA.

The tunnel layout is shown in Fig. 2. The settling chamber has a cross section of 212 mm x 212 mm and a length of 310 mm. It was fabricated from four cast pieces of aluminium which were machined, anodized and welded together. There are flow straighteners inside the settling chamber which consist of 5 mm diameter tubes of 100 mm length. Screens ( 10 mesh per cm ) are provided after the flow straighteners. A 25 mm strut is fitted in the central part of the settling chamber to assist central location of a nozzle for coaxial jet flows. The contraction ratio of the settling chamber is 9.2. The flexible air supply pipe is connected to the settling chamber through a short diverging pipe. The tunnel was mounted on a uniaxial precision traverse table (Fig. 2 ). The traverse table is fitted with a digital counter which has an accuracy upto 0.25 mm. A longitudinal slide support

is provided under the test section for facilitating and guiding the axial traverse of the tunnel.

The air supply to the tunnel is taken from the compressed air bottles of the trisonic tunnel. A 63 mm pipeline is laid for the supply of the compressed air to the tunnel. The arrangement consists of a two stage pressure regulation, pneumatic flow rate control, flow meter and various pressure gauges. The air supply to the nozzle passes through a DISA 55L17 seeding generator. The surrounding air stream is seeded using a TSI model 9306 six jet atomizer. The pressure and air flow rates to the seeding generators are separately controlled. A mixture of glycerin and water ( 50 % each ) was used in both the seeding generators.

The LDA set-up consists of a 16 mW He-Ne laser with a beam diameter of 1.1 mm. DISA 55L01 beam splitter was used to split the laser beam . The laser beam is made to intersect at the point where the measurement is to be done. The intersection of the beams take place at an angle of 23.04 degrees. The receiving optics consists of 55 x 08 photo multiplier (PM) section. The optical unit is mounted on a traverse system which enables data acquisition in the radial direction. DISA 55L15 high voltage supply gives a continuous High voltage supply to the photo multiplier. Voltage indication is provided by a front-panel meter. Another front-panel meter reads PM-tube anode current. The anode current depends on the amount of light reaching the PM tube and on the high voltage supply of the photo multiplier. Recommended anode current is 50  $\mu$ A, useful range from 10 to 100  $\mu$ A.

Doppler signal is processed using a Dantec 55L90 counter processor with a frequency range of 50 MHz. It is basically an "electronic stop-watch" which measures the time it takes for a particle to cross a known number of interference fringes in the measuring volume. The distance between the fringes is known from the geometry of the optical beams and the wavelength of the laser beam. The light scattered from the seeding particles is detected, and the result is a frequency-modulated current burst from the detector. The incoming photodetector signal is amplified 35 dB and band-pass filtered in the filter board. The pass band is selectable with the HIGH-PASS and the LOW-PASS selector knobs on the 55L96 COUNTER module front panel. DISA 55L94 MEAN VELOCITY COMPUTER module has two digital displays on the front panel showing mean velocity in scientific notation. These two displays are designated m/sec and POWER OF 10, respectively. The mean velocity is calculated by it on the basis of a number of validated velocity samples. DISA 55L91 DATA RATE module indicates the rate of validated data, and the number of validated data based on groups of 1000 bursts.

An ECIL oscilloscope was used to observe the nature of Doppler signal coming from the frequency tracker. The oscilloscope has a range of 50 MHz.

The counter processor is interfaced with a HCL PC-AT computer using a 1400A data acquisition interface. A full range of standard software is available for processing the acquired LDA data. Measurements were carried out in forward scatter mode. The



jet diameter was 1.8 mm and the jet flow was through a specially machined nozzle which has an outer diameter of 4 mm (Fig. 3). The free stream turbulence in the secondary flow was generated by placing a suitable grid between the contraction and the inlet of the test section.

## RESULTS AND DISCUSSION

Fig. 4 shows the distribution of the centre-line velocity with axial distance. Mean axial velocity is non-dimensionalised using issuing velocity (  $U_o$  ) and the axial distance (  $x$  ) using nozzle exit diameter (  $d$  ).  $U_c/U_o$  versus  $x/d$  for the velocity ratios 0.11, 0.22 and 0.33 are shown with free stream turbulence approximately 1.2 %. Fig. 5 shows the variation of  $U_c/U_o$  versus  $x/d$  for velocity ratios 0.11, 0.22, 0.33. Here, the average free stream turbulence is 10.5 %. As expected, the higher velocity ratios have higher  $U_c/U_o$  at a given  $x/d$ .

A comparison of  $U_c/U_o$  versus  $x/d$  at velocity ratio 0.22 and free stream turbulence 1.2 % was made between constant area mixing and variable area mixing, in Fig. 6. It is seen that  $U_c/U_o$  value for varying area is less than for constant area beyond  $x/d$  of 25. This indicates that for variable area mixing, decrease in centre-line velocity is more rapid. This result is in accordance with the result obtained by Choi et. al (14).

Fig. 7 shows the comparison of  $U_c/U_o$  versus  $x/d$  for free stream turbulence 1.2 % and 10.5 % for a velocity ratio of 0.22. It is seen that the centre-line velocity decays faster when it has a lower free stream turbulence.

Fig 8 shows the distribution of streamwise turbulence on the centreline with  $x/d$  for velocity ratios 0.11, 0.22 and 0.33. No grid is used and the average free stream turbulence is 1.2 %. The turbulence increases with  $x/d$  initially and attains a maximum

value of 0.199 at  $x/d$  of 13 and then it decreases. The turbulence level are higher at lower velocity ratios.

In Fig. 9 turbulence is plotted versus  $x/d$  with average free stream turbulence of 10.5 %. The distribution is shown for the velocity ratios of 0.11 and 0.33. The turbulence increases and attains a maximum value of 0.171 at  $x/d$  of 10. The turbulence level is higher for lower velocity ratios. The similar result is also given by (17).

Fig. 10 shows the variation of turbulence in the axial direction at the velocity ratio of 0.22. The comparison is made between constant area mixing and variable area mixing at a free stream turbulence of 1.3%. It is seen that in the variable area mixing the turbulence has a lower peak value as compared to the case of constant area mixing and the value of turbulence is less upto  $x/d$  of 15 for variable area mixing.

Fig. 11 shows the variation of turbulence along the axis for a velocity ratio of 0.11 and a free stream turbulence of 10.5%. It shows that the streamwise turbulence intensity for constant area mixing is higher than for variable area mixing for all  $x/d$  locations. The maximum value of turbulence intensity for constant area mixing is 20.5% at  $x/d$  10 and for variable area mixing it is 17.1% at  $x/d$  of 10.

Fig. 12 shows the decay of centreline velocity with respect to the  $x/d$  location. The free stream turbulence is 1.3% and the velocity ratios taken are 0.11, 0.22 and 0.33. Fig. 13 shows the decay of centreline velocity along the axial direction at velocity ratios 0.11, 0.22, and 0.33. The average free stream turbulence is

10.5%. These plots indicate that in the flow fields with lower velocity ratios the velocity decay is faster.

Fig. 14 shows the variation of  $(U_c - U_f)/(U_o - U_f)$  vs  $x/d$  at a velocity ratio of 0.22 for free stream turbulence of 1.2% and 10.5%. The plot indicates a faster decay in the velocity defect for higher free stream turbulence. This indicates higher mixing for higher free stream turbulence.

Fig. 15 shows the decay of velocity defect with  $x/d$  having free stream turbulence of 1.5% for constant area mixing and 1.2% for variable area mixing. The velocity ratio is 0.11. This plot indicates a higher velocity defect for flow having adverse pressure gradient.

Variation of jet half radius ( $R_{1/2}$ ) with  $x/d$  location is shown at an average free stream turbulence of 1.2% in Fig. 16. The velocity ratios taken are 0.11, 0.22 and 0.33. It is seen that flows with lower velocity ratio have larger jet radius and vice versa. A similar result is shown by (7) and (11).

Fig. 17 shows the variation of jet half radius along the axial direction at the velocity ratio of 0.33. The comparison is made between the jet radius with free stream turbulence of 1.2% and 10.5%. The plot indicates that at a particular velocity ratio, high free stream turbulence leads to a larger jet radius.

Fig. 18 shows the variation of  $R_{1/2}$  along the axial distance at velocity ratio of 0.11. The comparison is made between mixing at constant area at free stream turbulence 1.79% and mixing at variable area at free stream turbulence of 1.27%. The jet radius in the diverging test section is larger than the jet radius in the uniform area duct.

Fig. 19 shows the variation of mean velocity along the radial direction at a velocity ratio of 0.15 with free stream turbulence of 10.8%. The velocity distribution is shown at  $x/d$  distances of 10, 20, 30, 40, 50 and 60. For  $x/d$  of 10 there is a distinct demarcation between the jet and the free stream flow. This demarcation is seen by the velocity difference between primary and secondary flow which is almost discontinuous. This promotes more active momentum transfer and leads, in turn, to a more rapid spread of mixing layer. As we go downstream it is seen that the demarcation becomes less apparent and the velocity profile approaches to a fully developed flow.

The flow field region is not exactly two dimensional. The test section has a divergence on upper and lower walls only so it forms a three dimensional flow field. One set of measurements are made in the plane of divergence with pitot tube. We couldn't use LDA due to the limitations in the traverse system.

Fig. 20 shows the variation of mean velocity in the plane of divergence at a velocity ratio of 0.15 and a free stream turbulence of 10.3%. The velocity distribution is shown at  $x/d$  distances of 10, 20, 30, 40 and 50. This plot confirms the trend indicated by Fig. 19.

Fig. 21 shows the variation of mean velocity across the flow at a velocity ratio 0.11 and a free stream turbulence of 1.25%. The plot shows the variation of velocity at  $x/d$  distances of 10, 20, 30 and 40. This plot also indicates that the velocity drops very rapidly at  $x/d$  10 and 20. However, at  $x/d$  distances of 30 and 40 the velocity drop becomes more gradual.

Fig. 22 shows the variation of streamwise turbulence across the flow. The velocity ratio is 0.11 at a free stream turbulence of 1.25%. The turbulence variation is shown at the  $x/d$  distances 10, 20, 30 and 40. It is seen that the turbulence increases as we move away from the centre and attains a peak value, and then decreases as we move further away from the centre. However, the peak value shifts away from the centre and decreases as well as we move downstream. The peak value at  $x/d$  10 is 0.36 at  $Y/R_o$  of 2.8, at  $x/d$  20 it is 0.33 at  $Y/R_o$  of 4.2 and at  $x/d$  40 the peak value of turbulence is 0.28 at  $Y/R_o$  of 5.6.

The variation of streamwise turbulence across the flow at a velocity ratio of 0.22 and free stream turbulence of 1.3% is shown in Fig. 23. The maximum value of turbulence at  $x/d$  of 10 is 0.28 at  $Y/R_o$  of 2.8. The value at  $x/d$  of 20 is 0.21 at  $Y/R_o$  of 3.5. If we compare with Fig. 22 it indicates that the peak turbulence value decreases as we increase the velocity ratio and the peak shifts towards the centre at a particular  $x/d$ . A similar result is obtained by (17).

Fig. 24 shows the variation of streamwise turbulence in the radial direction for a velocity ratio at 0.15 at a free stream turbulence of 10.8%. Fig. 25 shows the variation of streamwise turbulence across the flow at a velocity ratio of 0.33 at a free stream turbulence of 9.7%. They show that the peak turbulence decreases and the peak turbulence intensity shifts away from the centre as we move downstream. For the same grid the flow with higher velocity ratio has lower turbulence and its peak value. The peak shifts towards the centre for higher velocity ratio provided other conditions are identical.

Fig. 26 shows the variation of turbulence in the radial direction for velocity ratio of 0.15 at a free stream turbulence of 10.8%. A comparison is made for constant area mixing and variable area mixing. For  $x/d$  of 20, the value of turbulence is 0.24 and 0.254 for variable area and constant area mixing respectively. For  $x/d$  of 20 it is 0.164 and 0.205 having peak values at  $Y/R_o$  of 3.5 and 5.56 for variable area and constant area mixing respectively. At  $x/d$  of 40 value of maximum turbulence is 0.143 and 0.153 for variable area mixing and constant area mixing respectively. Their respective peak values lie at  $Y/R_o$  of 5.6 and 6.94. Hence it is seen that in the constant area mixing the value of turbulence are slightly higher and peak shifts away from the centre.

In Fig. 27 the turbulent component of streamwise velocity  $U_{rms}$  is normalised with the velocity defect ( $U_c - U_f$ ) and is plotted versus  $Y/R_{1/2}$ . The velocity ratio is 0.11 and the free stream turbulence is 1.25%. The turbulent intensities are plotted at  $x/d$  of 10, 20 and 30. The peak value of  $U_{rms}/(U_c - U_f)$  increases as we go downstream. For  $x/d = 10$ , the peak value is 0.251 at  $Y/R_{1/2}$  of 0.4. The maximum values at  $x/d$  20 and 30 are 0.276 at  $Y/R_{1/2}$  of 0.5 and 0.287 at  $Y/R_{1/2}$  of 0.6 respectively. This indicates that as we go downstream the peak value increases as well as shifts away from the centre.

In Fig. 28 variation of  $U_{rms}$  intensity is shown for velocity ratio of 0.22 at a free stream turbulence of 10.5%. The  $x/d$  locations for which the data is presented are 10, 30 and 50. The maximum intensities at  $x/d$  of 10, 30 and 50 are 0.278 at  $Y/R_{1/2}$  of 0.40, 0.277 at 0.70 and 0.33 at 0.70 respectively.

In Fig. 29 variation of U-intensity is taken along the radial direction. The velocity ratio is 0.15 and the free stream turbulence is 10.5%. The intensity is measured at  $x/d$  distances of 10, 30, 50 and 60. This also shows similar trend as plots 23 and 24 have shown. (11) shows that the peak value of  $U_{rms}/(U_c - U_f)$  increases as we move away from the centre.

Mean velocity similarity profiles are shown in Fig. 30 and 31. The velocity scale chosen is the velocity defect between the centreline velocity and the free stream velocity. The length scale chosen is  $R_{1/2}$ .  $R_{1/2}$  is the distance from the centreline along the radial direction where the mean velocity is  $0.5(U_c + U_f)$ . Fig. 30 shows the similarity profile at a velocity ratio of 0.11 and free stream turbulence of 1.27%. Fig. 31 shows the similarity profiles at a velocity ratio of 0.33 and a free stream turbulence of 1.15%.

Similarity profile at a velocity ratio of 0.15 is shown in Fig. 32 and Fig. 33 at a free stream turbulence of 10.8% and 10.3% respectively. In Fig. 33 the measurements are taken in the plane of divergence. This set of measurements is taken by pitot tube. It is seen that the plots at various  $x/d$  for a particular velocity ratio and free stream turbulence are self-similar.

Fig. 34 represents the similarity profile at a velocity ratio of 0.15 and free stream turbulence of 10.8% for constant area mixing. Here also, the profiles at various  $x/d$  locations are self-similar.



## Conclusions

Flow in the near field region of a jet issuing into a co-flowing stream is studied experimentally. Results for co-flowing jets mixing in a constant area duct are compared with the mixing under an imposed adverse pressure gradient. The experiments have been conducted at two different values of free stream turbulence and at several velocity ratios ranging from 0.1 to 0.33. Based on measurements, following conclusions can be drawn:

(a) The presence of an imposed pressure gradient in the streamwise direction results in more rapid decrease in the centreline velocity. However, in the initial mixing region, presence of imposed pressure gradient does not alter the profile of centreline velocity significantly.

(b) The rate of decay of the centreline velocity is higher for lower velocity ratio and for lower free stream turbulence levels.

(c) The jet half radius increases when an adverse pressure gradient in the streamwise direction is imposed.

(d) The peak value of turbulence at a given  $x/d$  location shifts away from the axis for variable area mixing. This indicates greater mixing at stations away from the axis. However, the value of maximum turbulence decreases for variable area mixing.

(e) Similarity in mean velocity profiles is observed across the flow, for both constant area mixing and variable area mixing. Flow similarity is observed for all velocity ratios and free stream turbulence values.

## BIBLIOGRAPHY

- (1) Landis, F. and Shapiro, A.H., *"The Turbulent Mixing Of Co-Axial Gas Jets"*, Proceedings Of Heat Transfer And Fluid Mechanics Institute, 1951, pp 133-146.
- (2) Curtet, R., *"Confined Jets And Recirculation Phenomenon With Cold Air"*, Combustion and Flame, Vol. 2, 1958, pp 383-411.
- (3) Curtet, R. and Ricou, F.P., *"On Tendency Of Self Preservation In Axi-Symmetric Ducted Jets"*, Journal of Basic Engineering, Vol. 86, 1964, pp 765-776.
- (4) Bradbury, L.J.S. and Riley, J. *"The Spread Of A Turbulent Plane Jet Issuing Into A Parallel Moving Air Stream"*, Journal Of Fluid Mechanics, 27, 1967, pp 381-397.
- (5) Durst, F. and Whitelaw, J.H., *"Measurement of Mean Velocity, Fluctuating Velocity And Shear Stress Using A Single Channel Anemometer"*, DISA Information, No. 12, 1971, pp 11.
- (6) *"Free Turbulent Shear Flows : Vol II-Summary Of Data"* Proceedings Of A Conference Held At NASA Langley Research Centre, Hampton, Virginia, July 1972.
- (7) Antonia, R.A. and Bilger, R.W., *"An Experimental Investigation Of An Axi-Symmetric Jet In a Co-Flowing Air Stream"*, Journal of Fluid Mechanics, Vol. 61, Part 4, 1973, pp 805-822.
- (8) Ramaprian, B.R. and Chandrasekhar, M.S., *"LDA Measurements In Plane Turbulent Air Jets"*, ASME - FE - 9.
- (9) Antonia, R.A. and Bilger, R.W., *"The Prediction Of The Axi-Symmetric Turbulent Jet Issuing Into A Co-Flowing Air Stream"*, Aeronautical Quarterly, Feb. 1974, pp 69-80.

- (10) Rodi, W and Spalding, D.B., "A Two-Parameter Model Of Turbulence And Its Application On Free Jets", *Warme-und Stoffubertragung*, Vol. 3, 1970, pp 85.
- (11) Smith, D.J. and Hughes, T., "Some Measurements In A Turbulent Circular Jet In The Presence Of A Co-Flowing Freestream", *Aeronautical Quarterly*, 1977, pp 185-196.
- (12) Habib, M.A. and Whitelaw, J.H., "Velocity Characteristics Of Confined Co-Axial Jets With And Without Swirl", *Trans of ASME, Journal of Fluid Engineering*, Vol. 102, 1980, pp 47-53.
- (13) Sullerey, R.K. and Chaldwade, C.D., "Measurements In Confined Jets With Varying Outer Stream Turbulence", *Proceedings of International Conference on Laser-Anemometry-Advances and Applications*, Manchester, 1985, pp 203-218.
- (14) Choi, D.W., Gessner, F.B. and Oates, G.C., "Measurements Of Confined Co-Axial Jet Mixing With Pressure Gradient", *Journal of Fluid Engineering*, Vol. 108, March 1986, pp 39-46.
- (15) Rajarathnam, N., "Turbulent Jets", Elsevier Publishing Company, NY, 1976, pp 27-49.
- (16) Singh, S.N., Agrawal, D.P., Malhotra, R.C. and Raghva, A.K. "Effect Of Swirl On Mixing Of Co-Axial Jets", *The Aeronautical Journal*, Vol 95, No. 943, 1991, pp 95-102.
- (17) Sullerey, R.K. "LDA Measurements In Co-Axial Jet Flows", *Final Report of Work Done Under ARDB Grant-In-Aid Scheme*, 1992.
- (18) So, R.M.C. and Aksoy, H. "Gas Jets In Arbitrary Stream", *The Aeronautical Journal*, Vol 197, No. 968, 1993, pp 287-295.
- (19) Kuhlman, J.M. and Gross, R.W., "Three Component Velocity Measurements In An Axi-Symmetric Jet Using LDV", *DANTEC Information*, No. 12, Feb. 1993, pp 10-16.

(20) Johnson, R.W. *"Prediction Of Turbulent Co-Axial Streams Of Constant And Variable Density"*, Journal Of Propulsion And Power, Vol. 9, No. 4, July-Aug. 1993, pp 588-596.

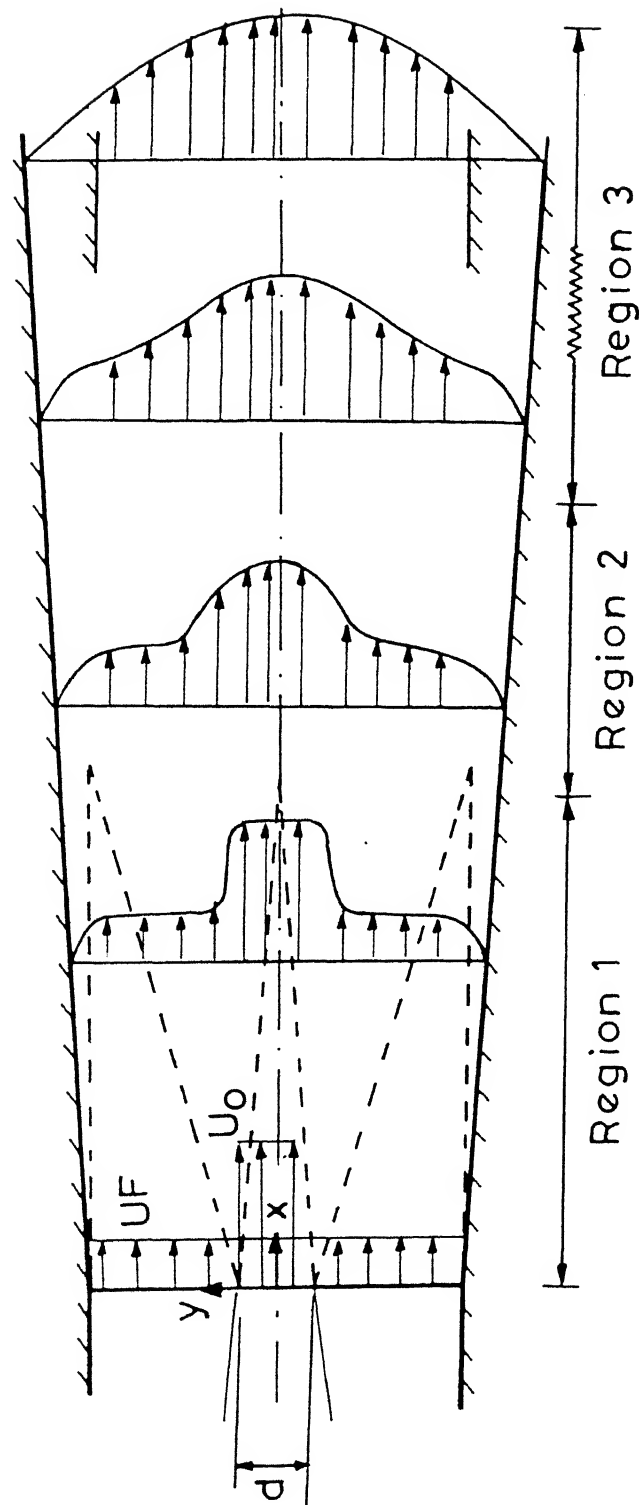


FIG.1. FLOW GEOMETRY

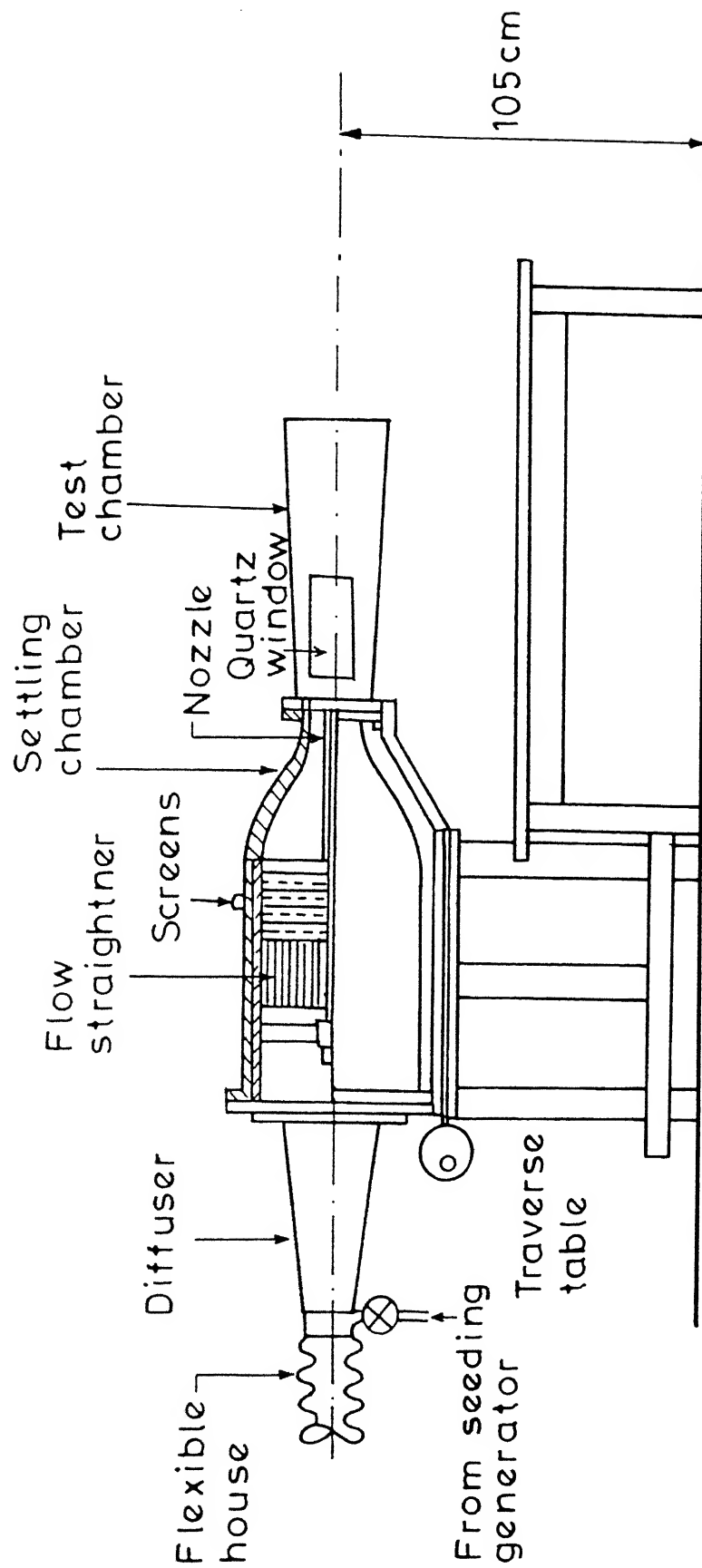


FIG.2. TUNNEL LAYOUT

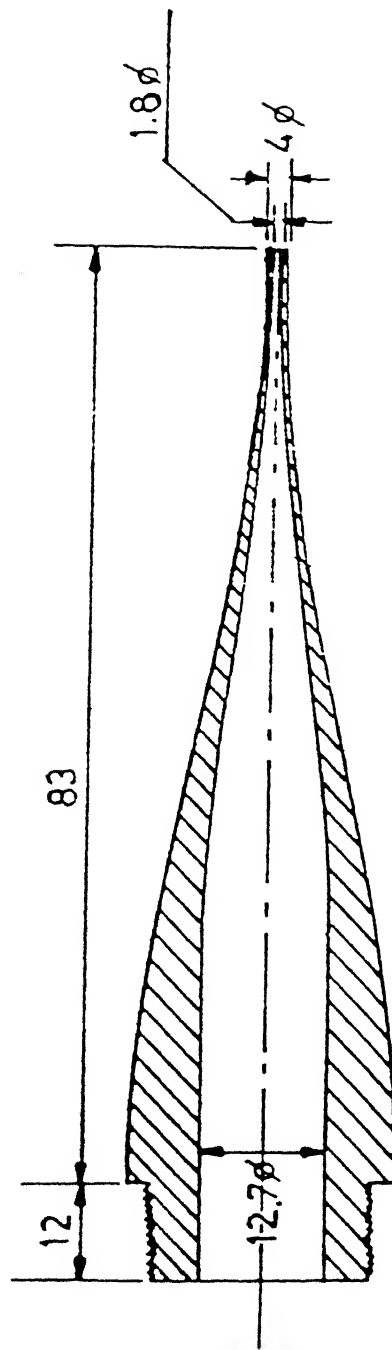


FIG. 3. NOZZLE

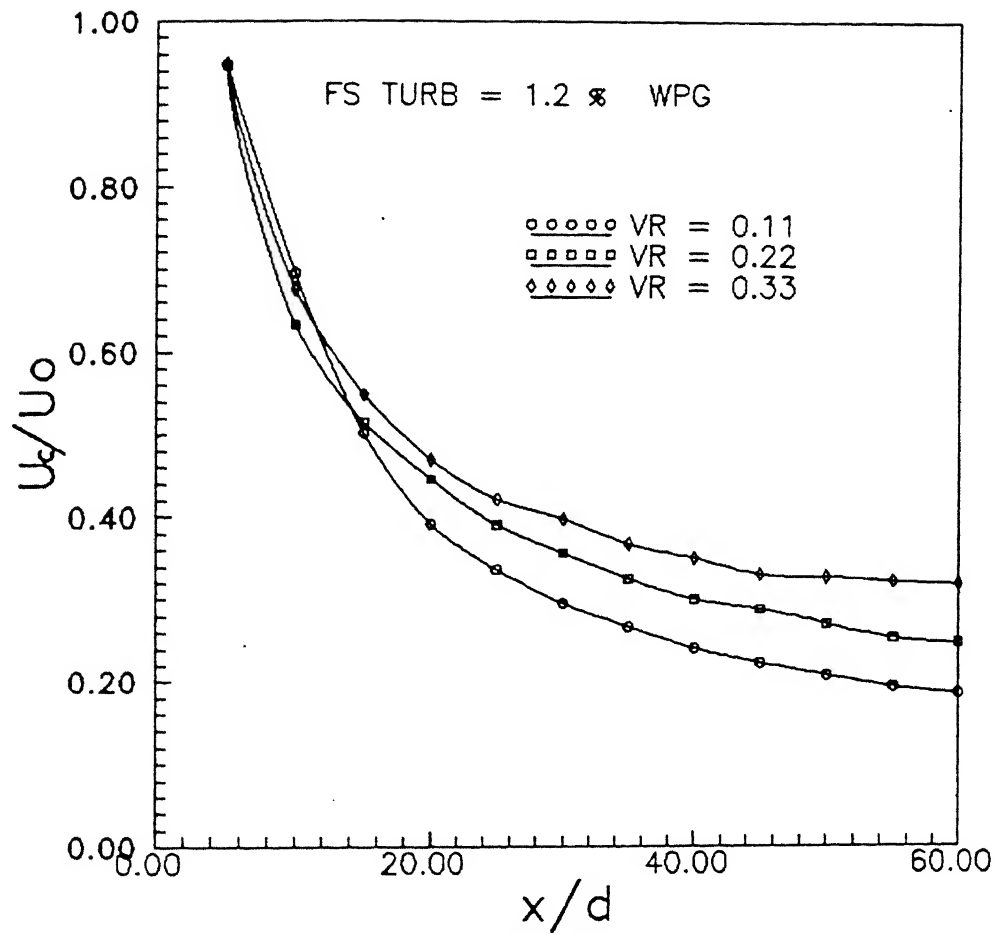


FIG. 4 AXIAL DISTRIBUTION OF CENTRELINE VELOCITY



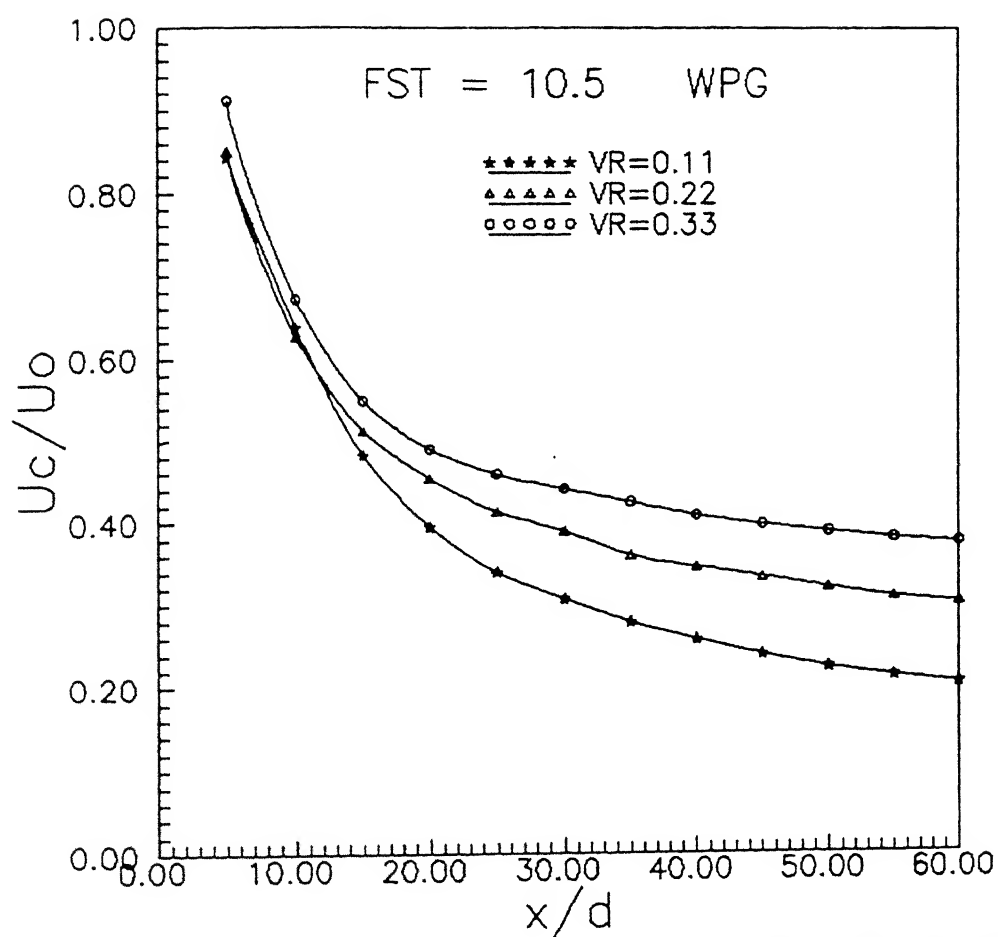


FIG. 5 AXIAL DISTRIBUTION OF CENTRELINE VELOCITY

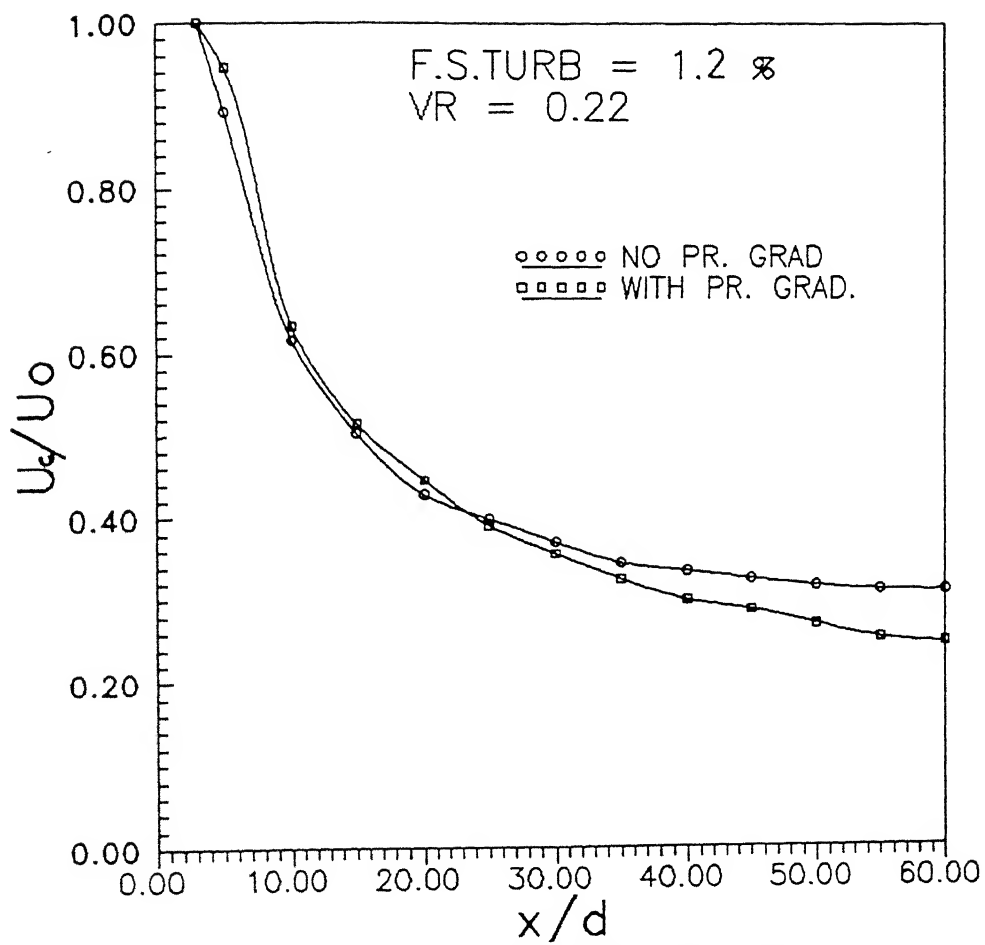


FIG.6. AXIAL DISTRIBUTION OF CENTRELINE VELOCITY

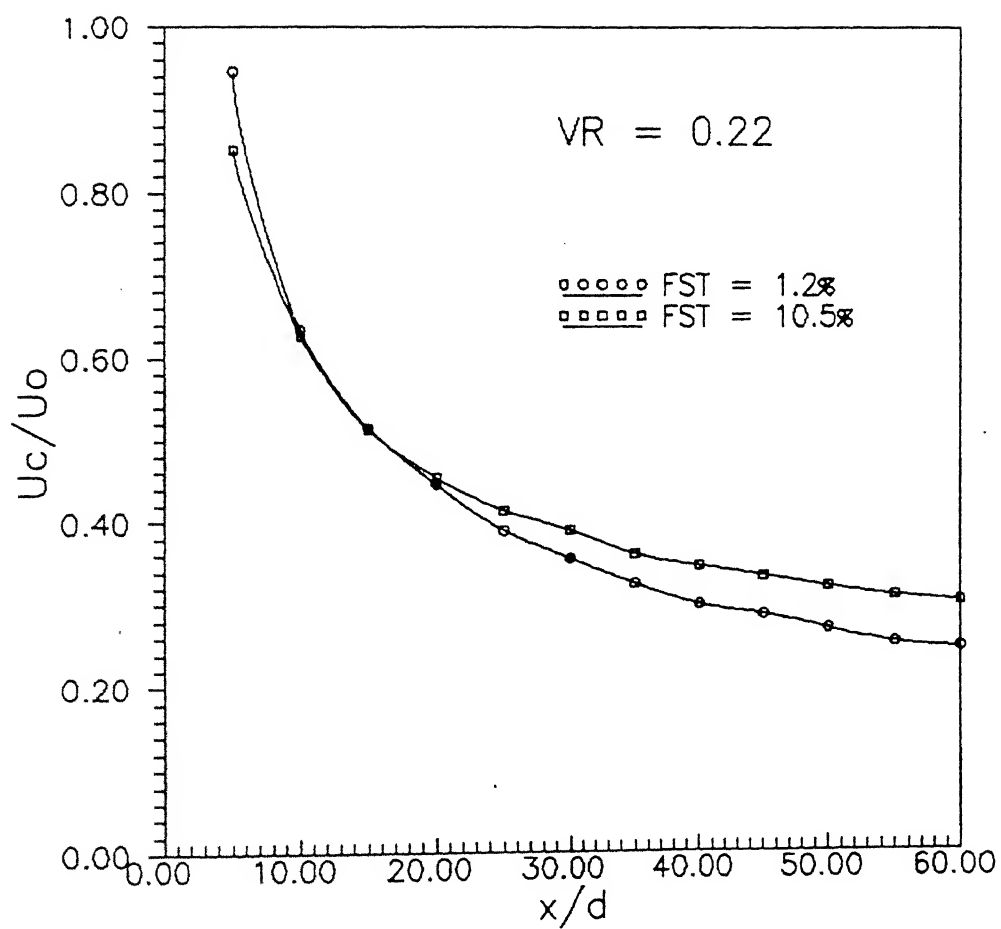


FIG. 7 AXIAL DISTRIBUTION OF CENTRELINE VELOCITY

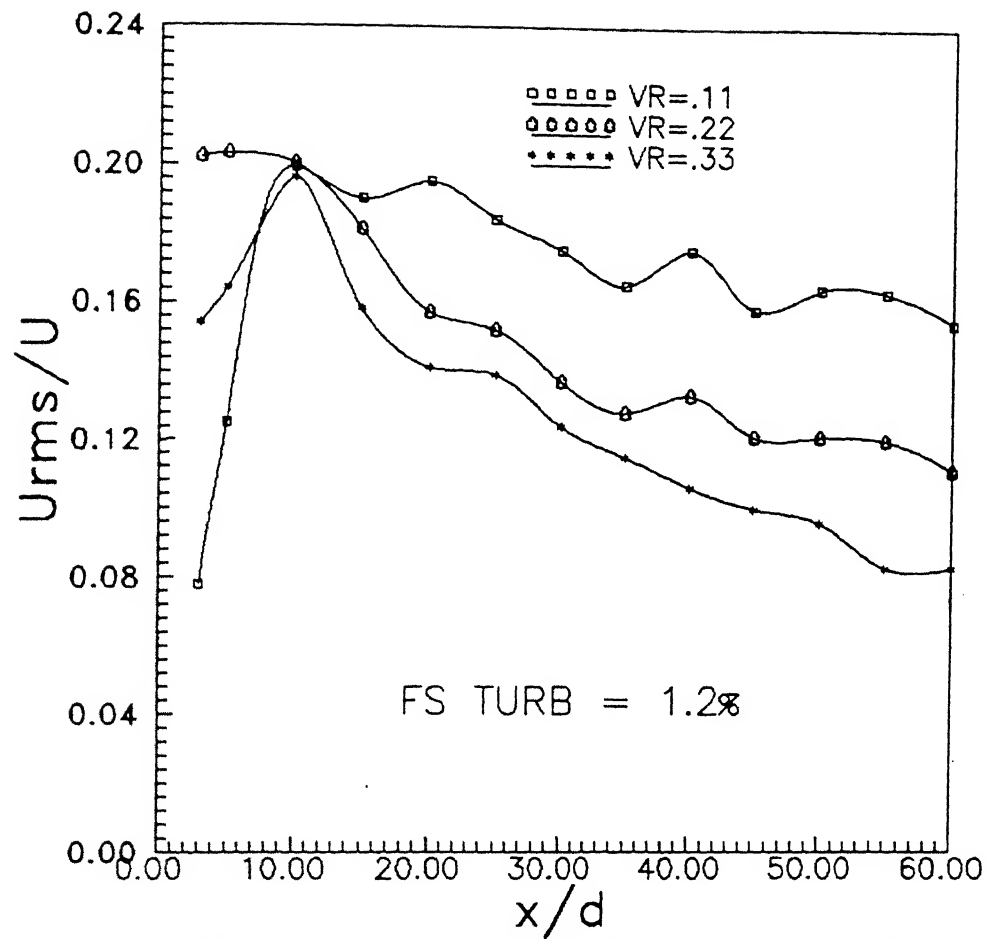


FIG. 8 AXIAL DISTRIBUTION OF STREAMWISE TURBULENCE

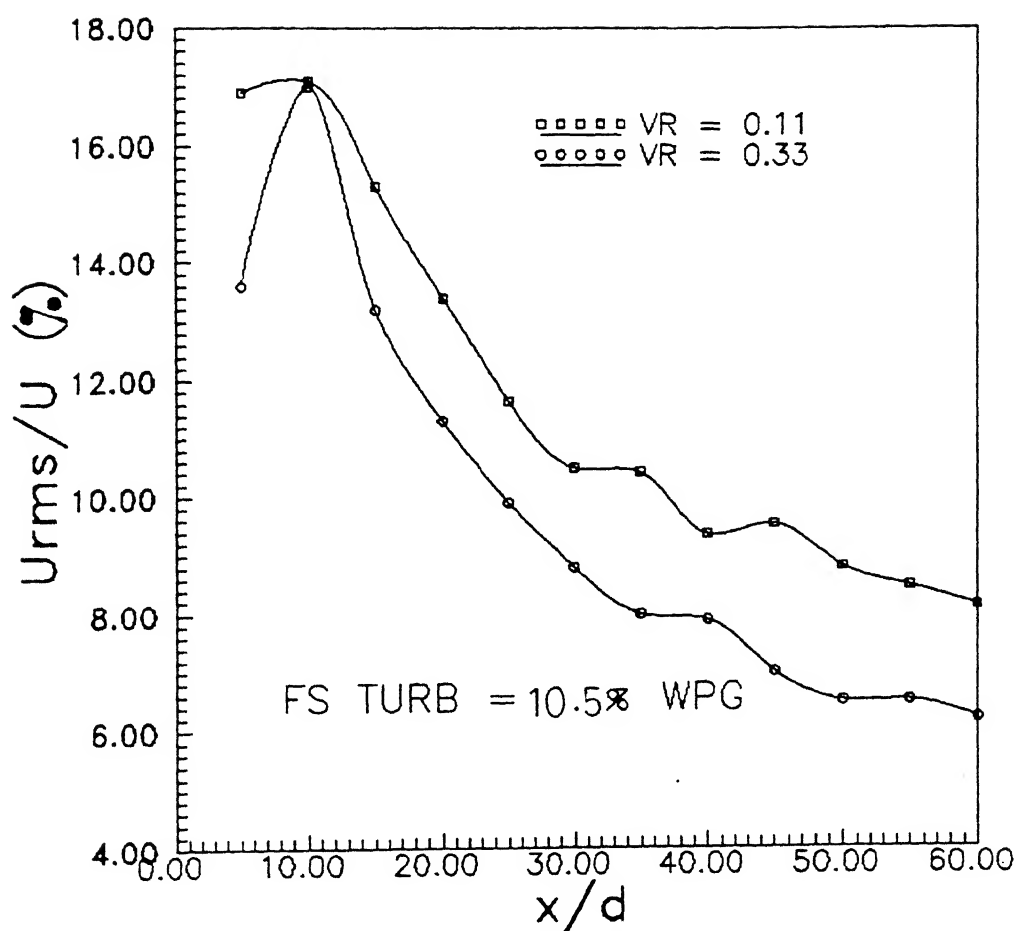


FIG. 9 AXIAL DISTRIBUTION OF STREAMWISE TURBULENCE

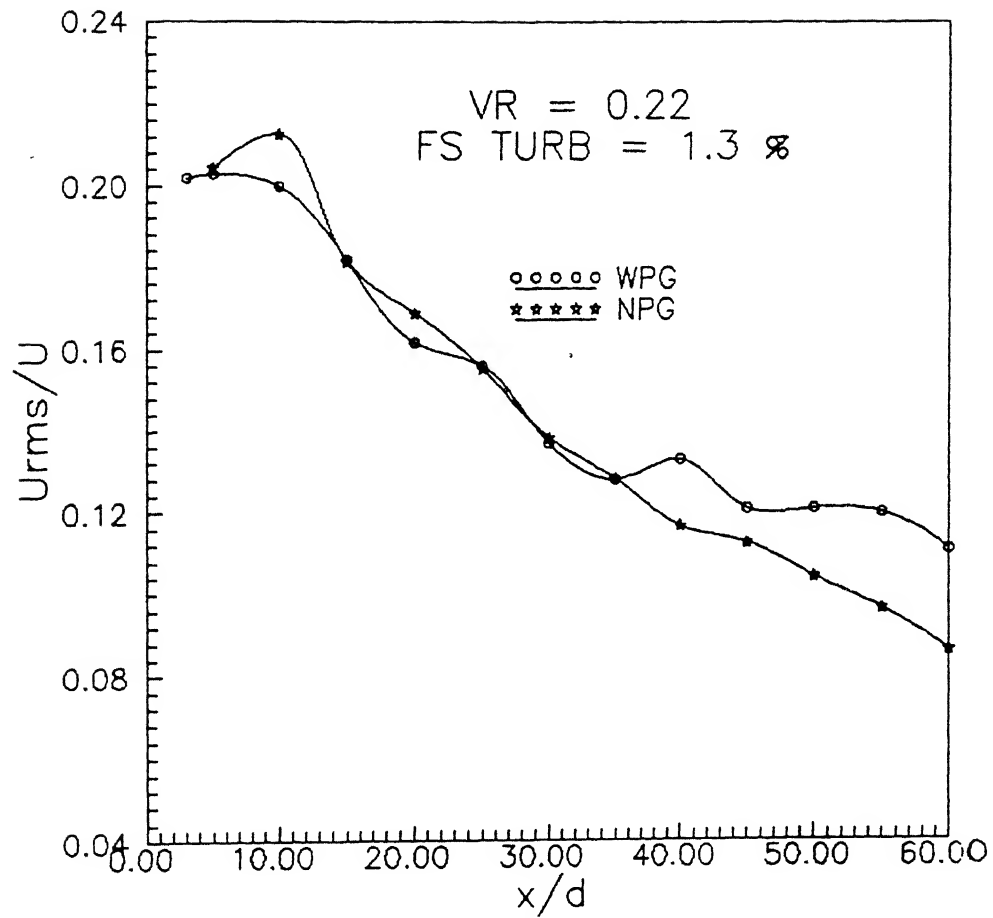


FIG.10 VARIATION OF STREAMWISE TURBULENCE ALONG THE AXIS

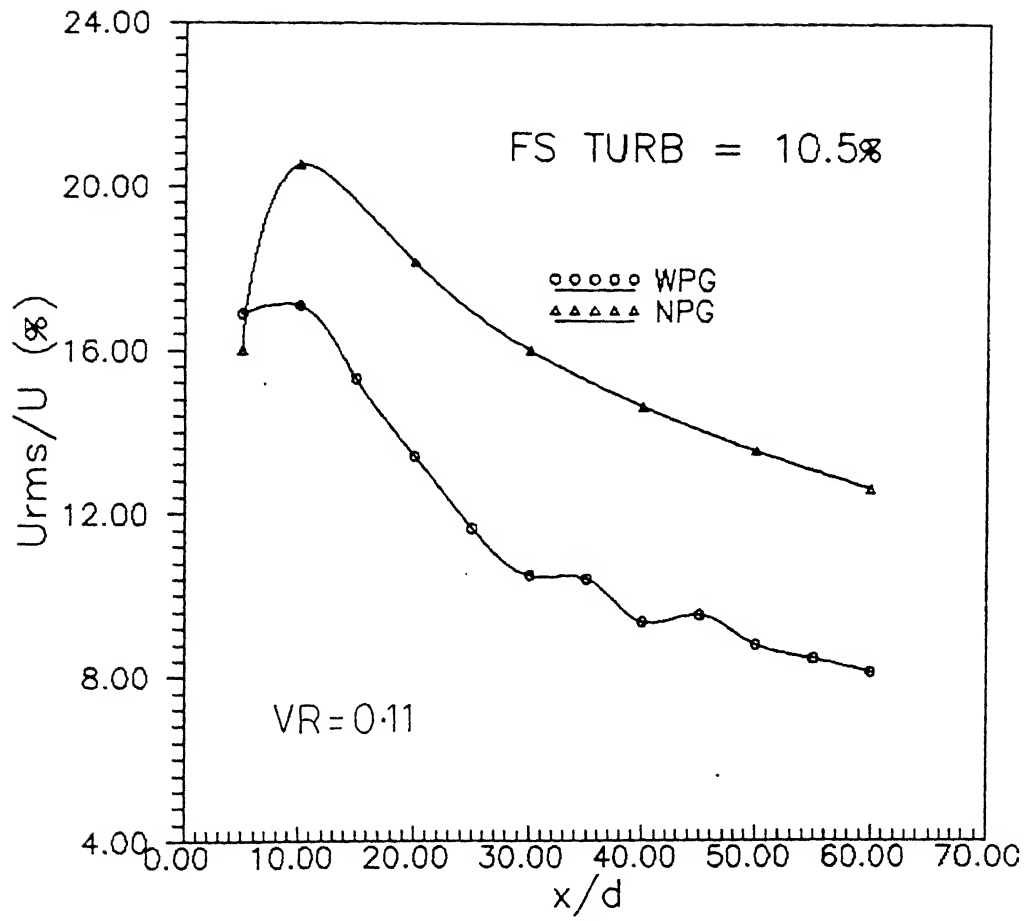


FIG.11 VARIATION OF STREAMWISE TURBULENCE ALONG THE AXIS

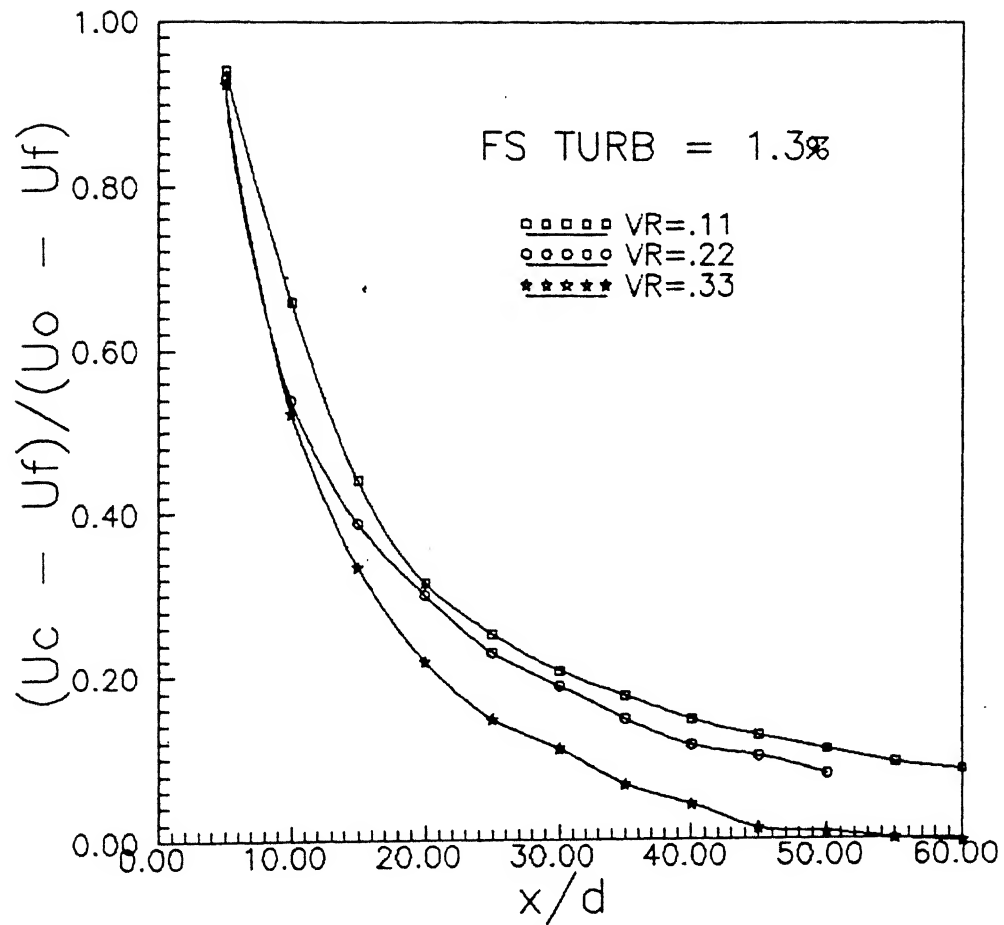


FIG.12 VARIATION OF VELOCITY DEFECT ALONG THE AXIS



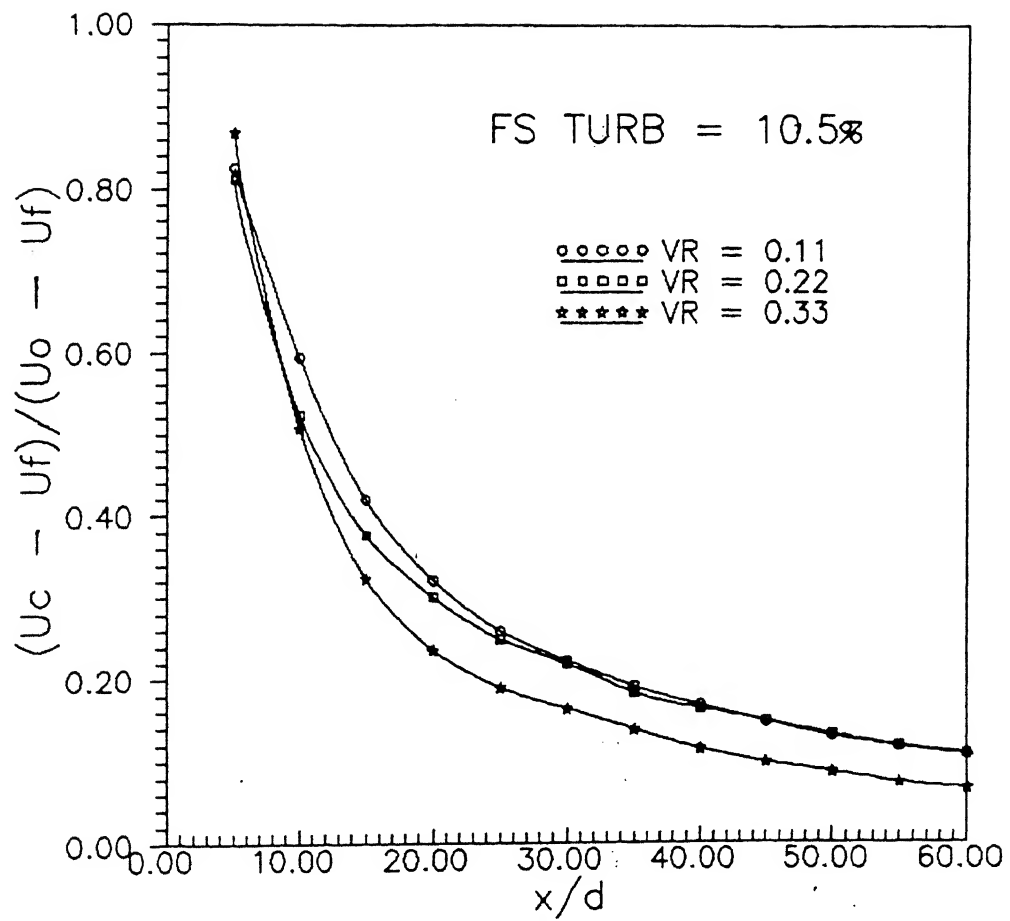


FIG.13 VARIATION OF VELOCITY DEFECT ALONG THE AXIS

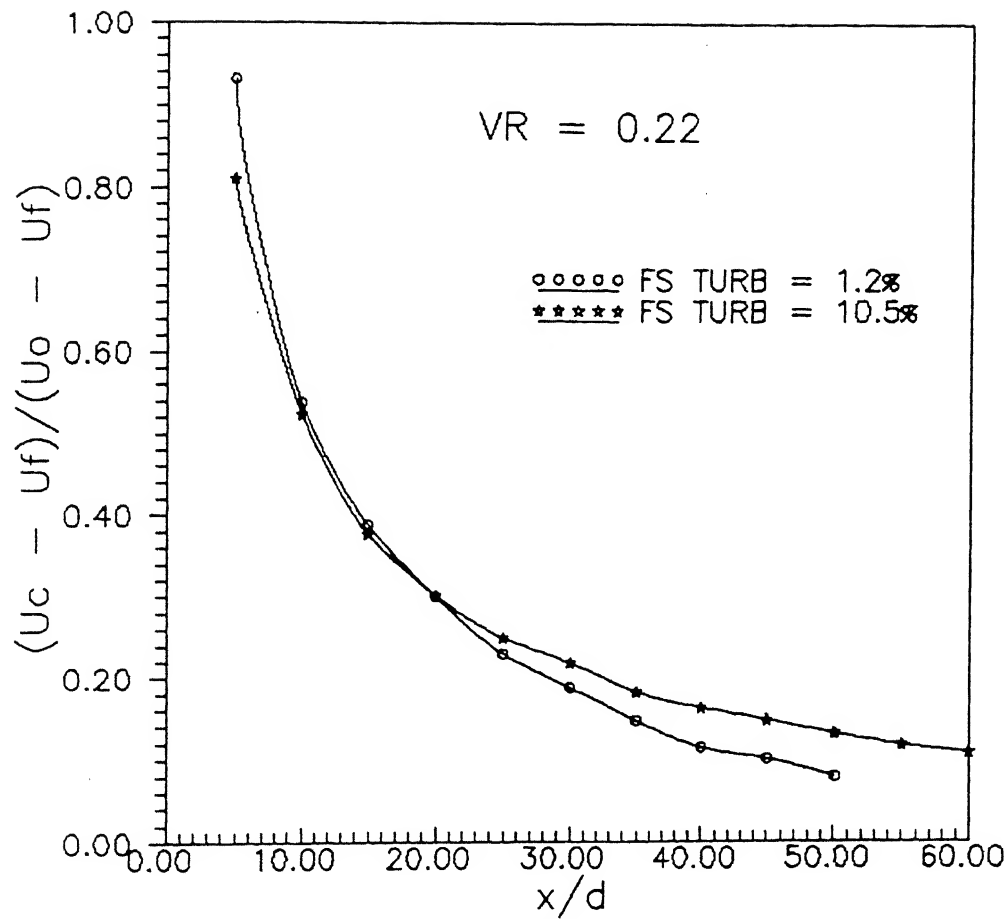


FIG.14 VARIATION OF VELOCITY DEFECT ALONG THE AXIS

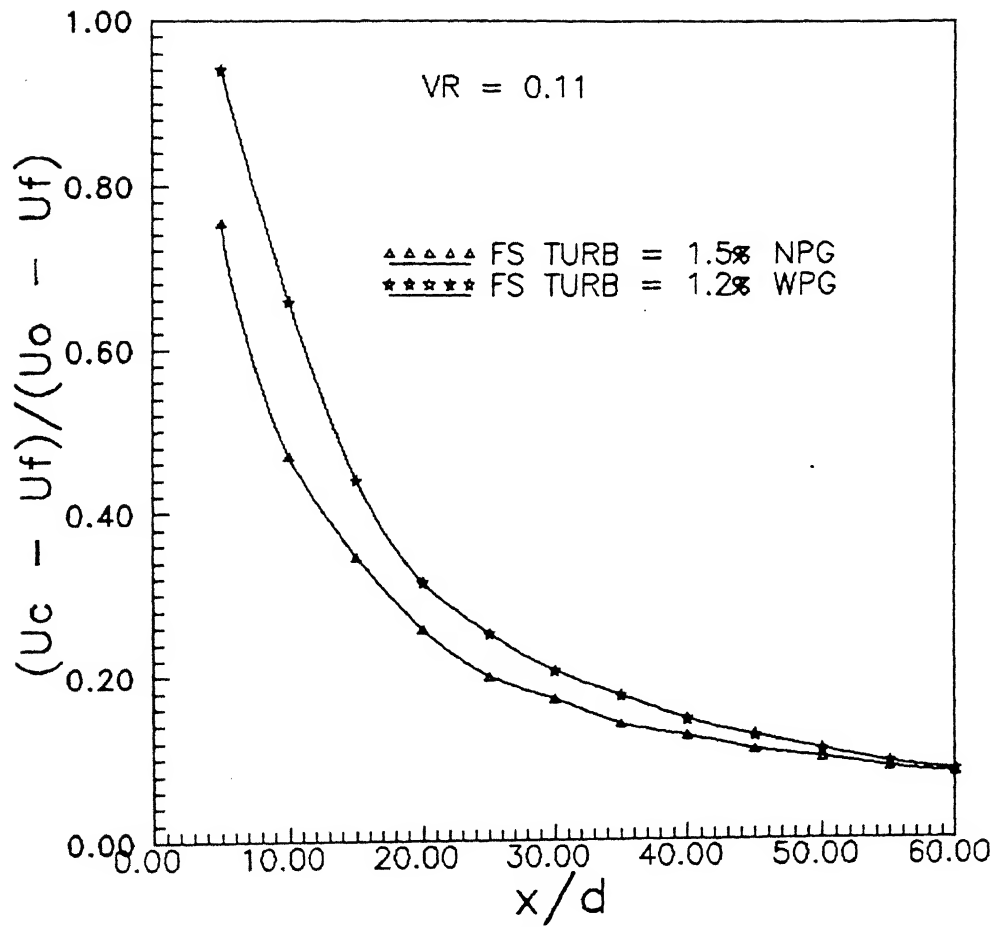


FIG.15 VARIATION OF VELOCITY DEFECT ALONG THE AXIS

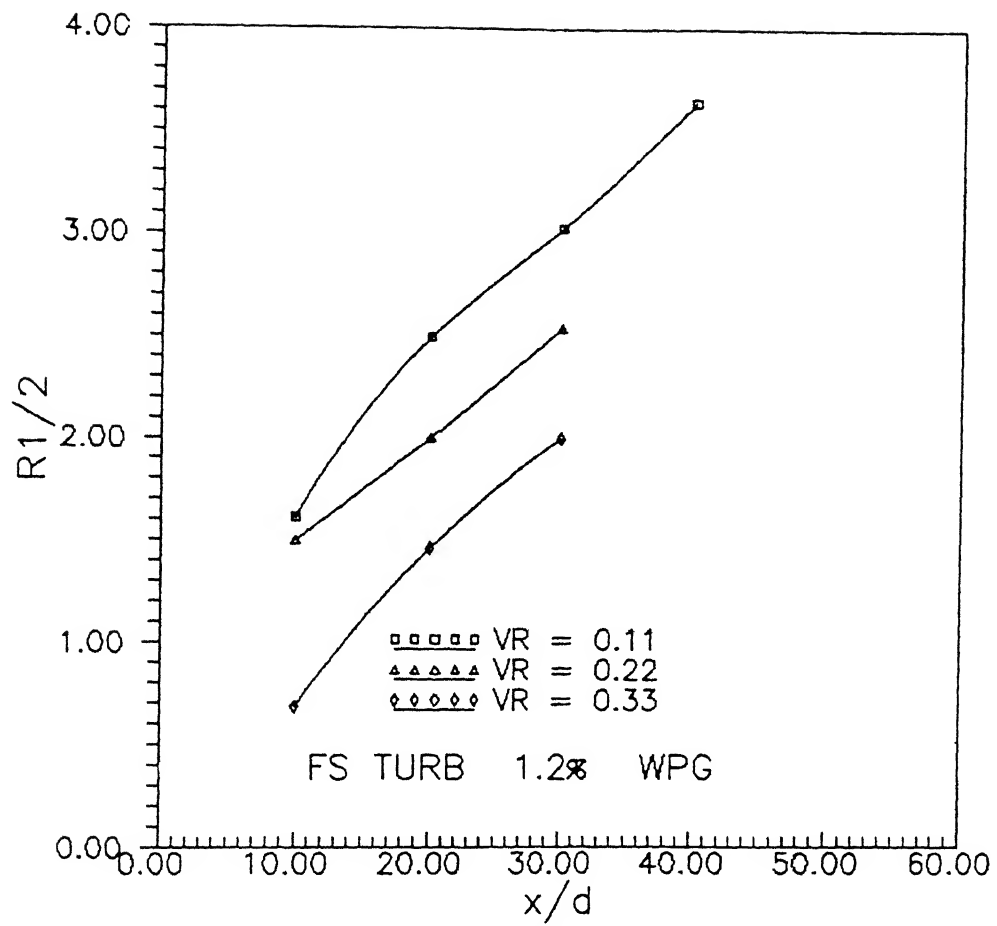


FIG.16 AXIAL DISTRIBUTION OF JET HALF RADIUS

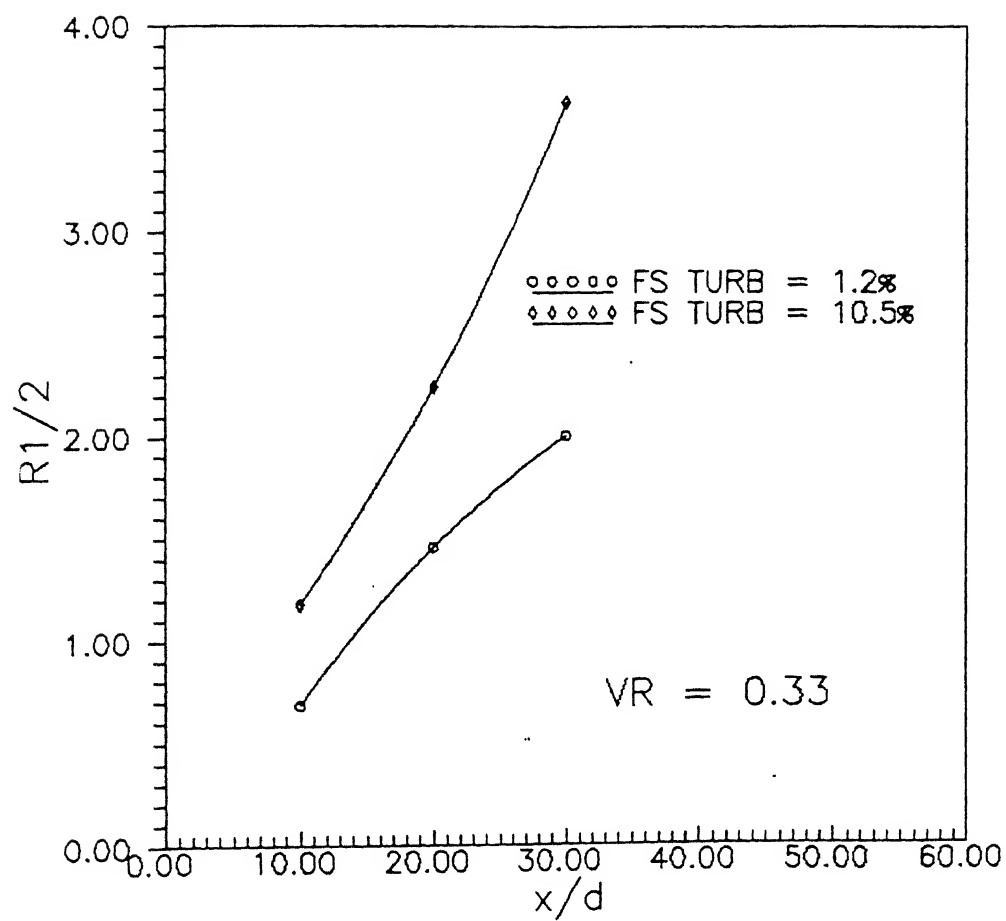


FIG.17 AXIAL DISTRIBUTION OF JET HALF RADIUS

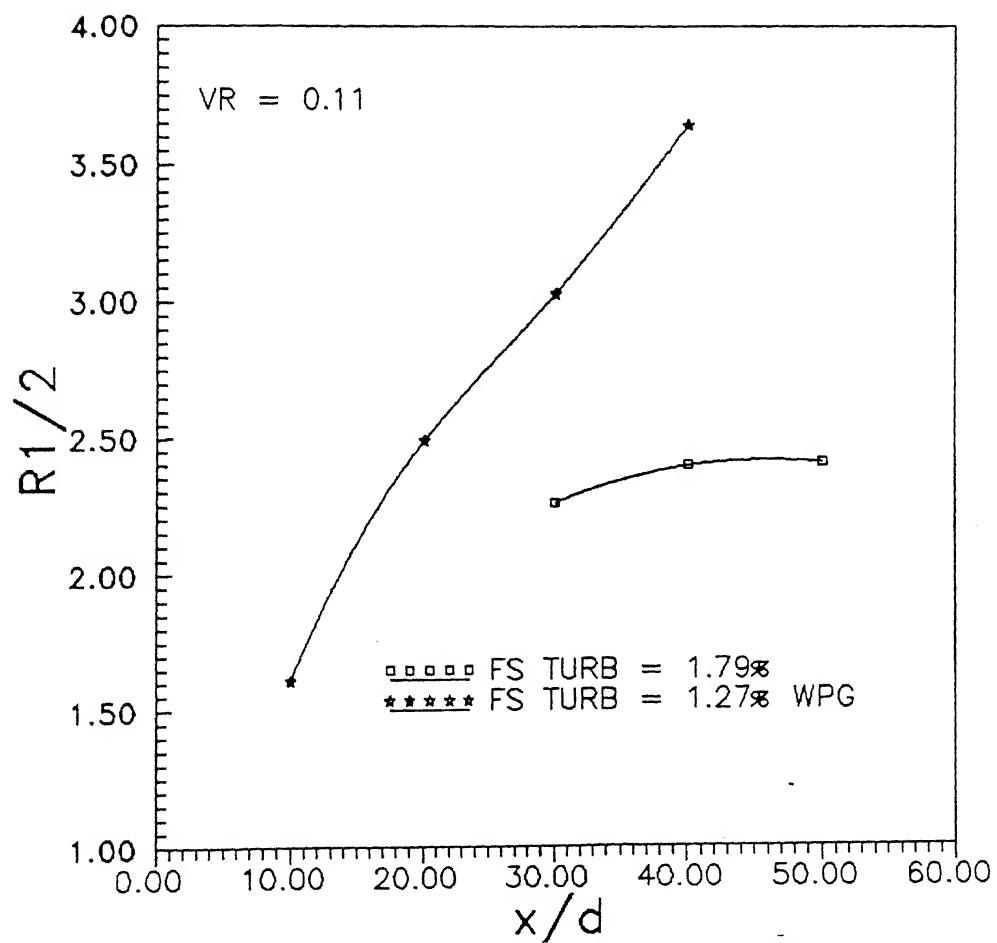


FIG.18. AXIAL DISTRIBUTION OF JET HALF RADIUS

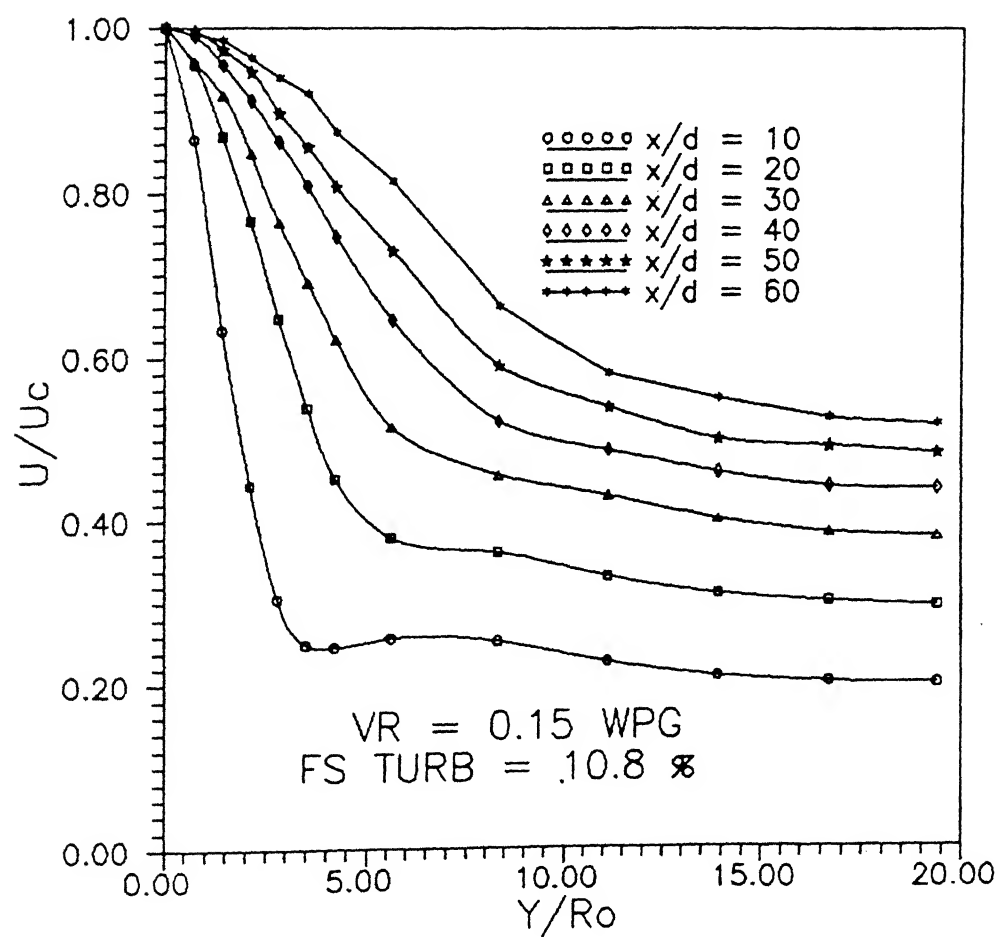


FIG.19. MEAN VELOCITY PROFILES ACROSS THE FLOW

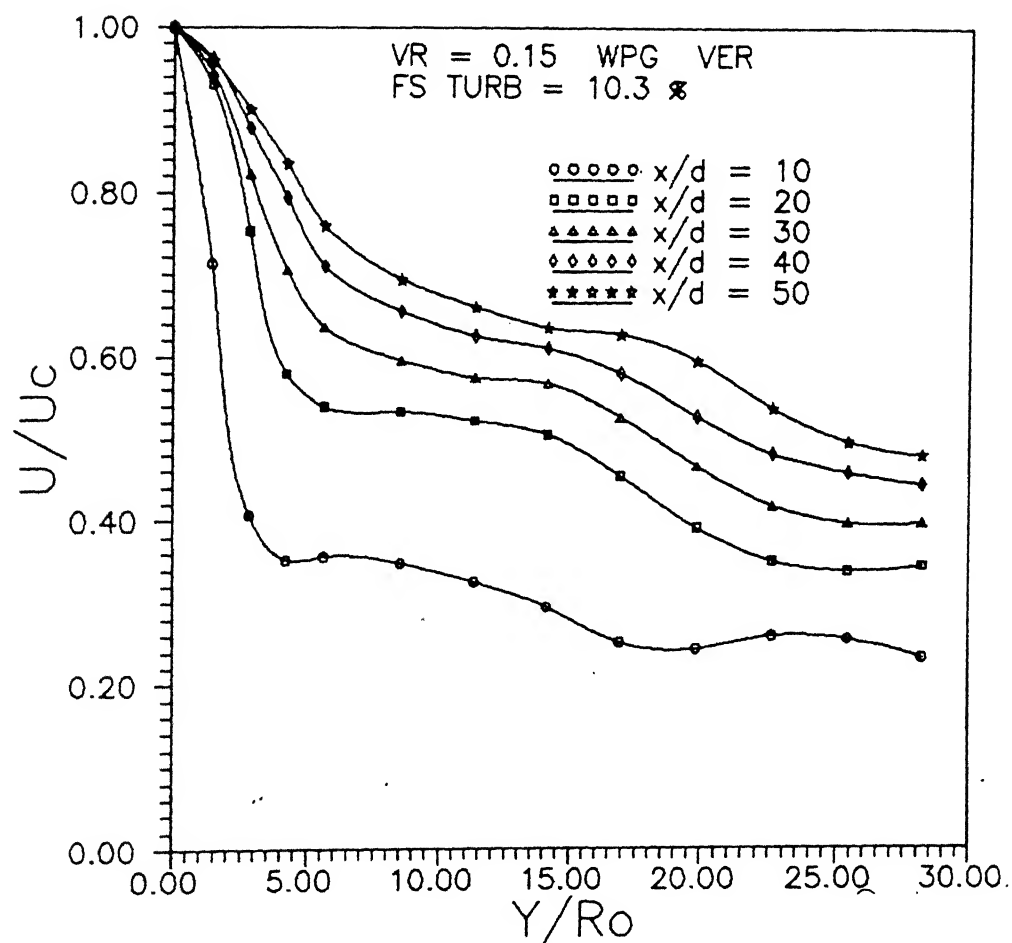


FIG. 20. MEAN VELOCITY PROFILES ACROSS THE FLOW



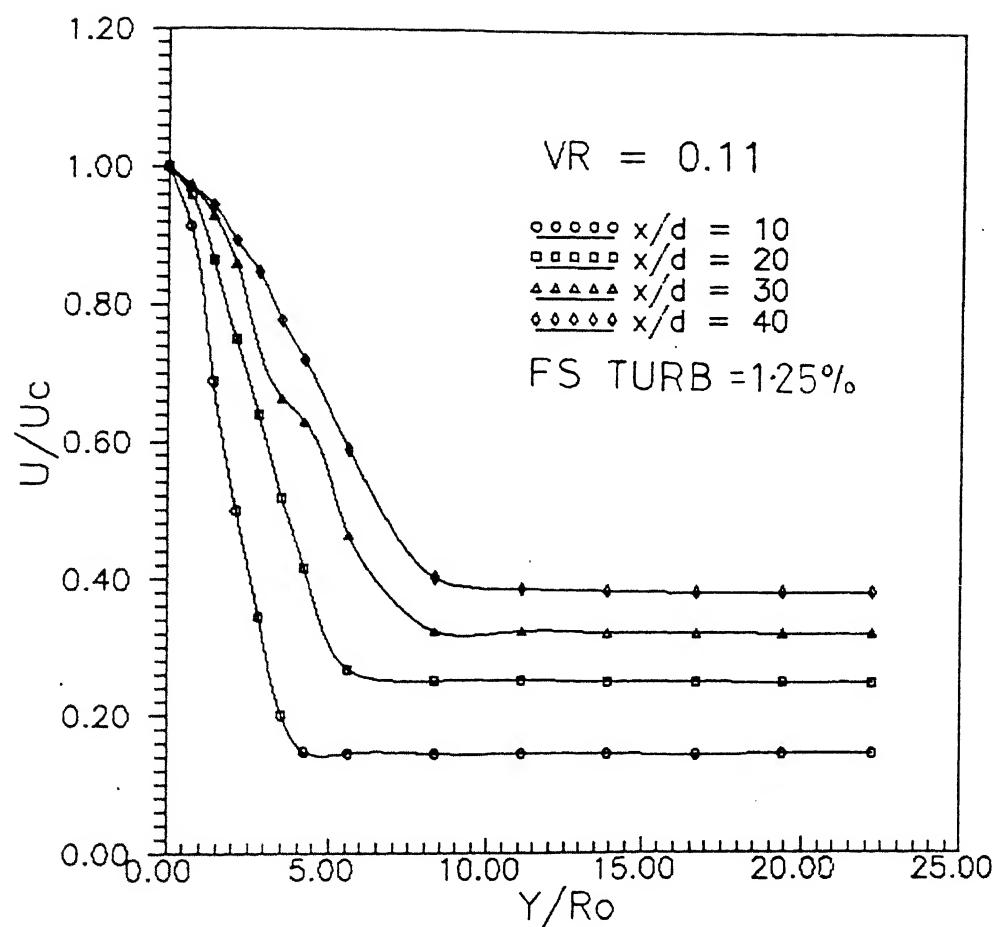


FIG.21 MEAN VELOCITY PROFILE ACROSS THE FLOW

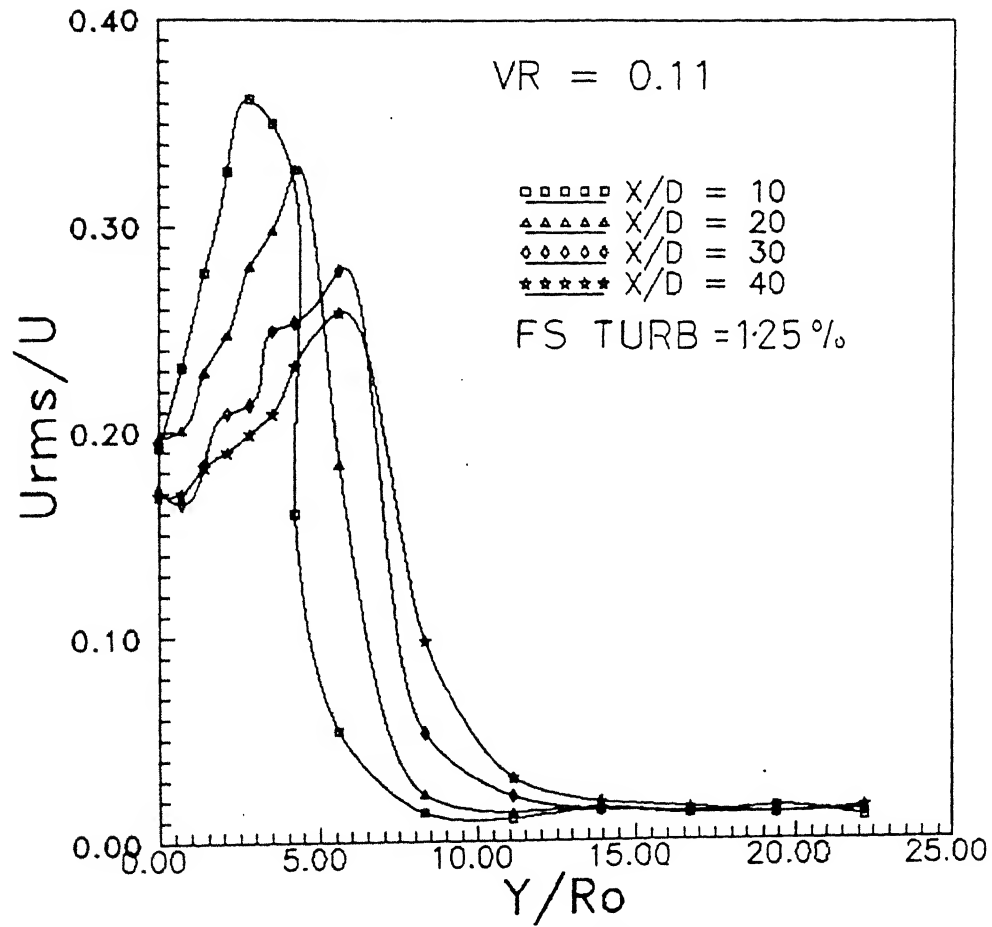


FIG.22 STREAMWISE TURBULENT INTENSITY ACROSS THE FLOW

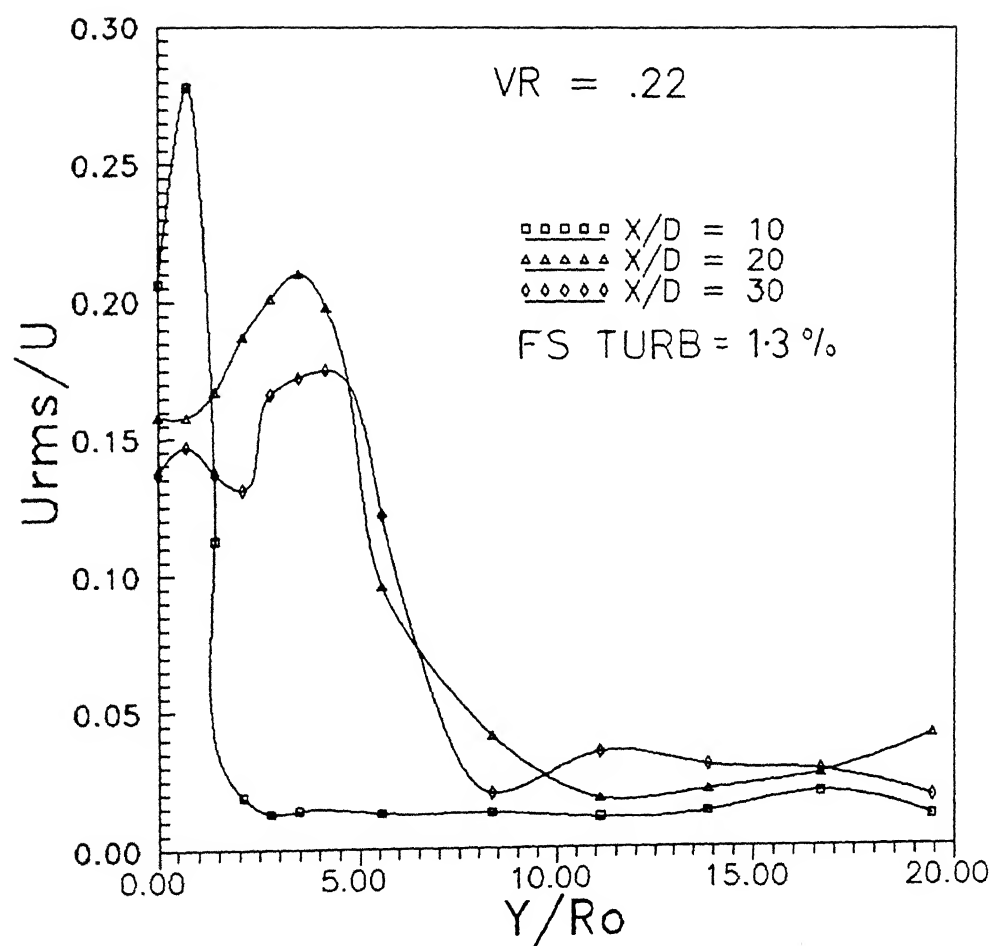


FIG. 23. STREAMWISE TURBULENCE INTENSITY ACROSS THE FLOW

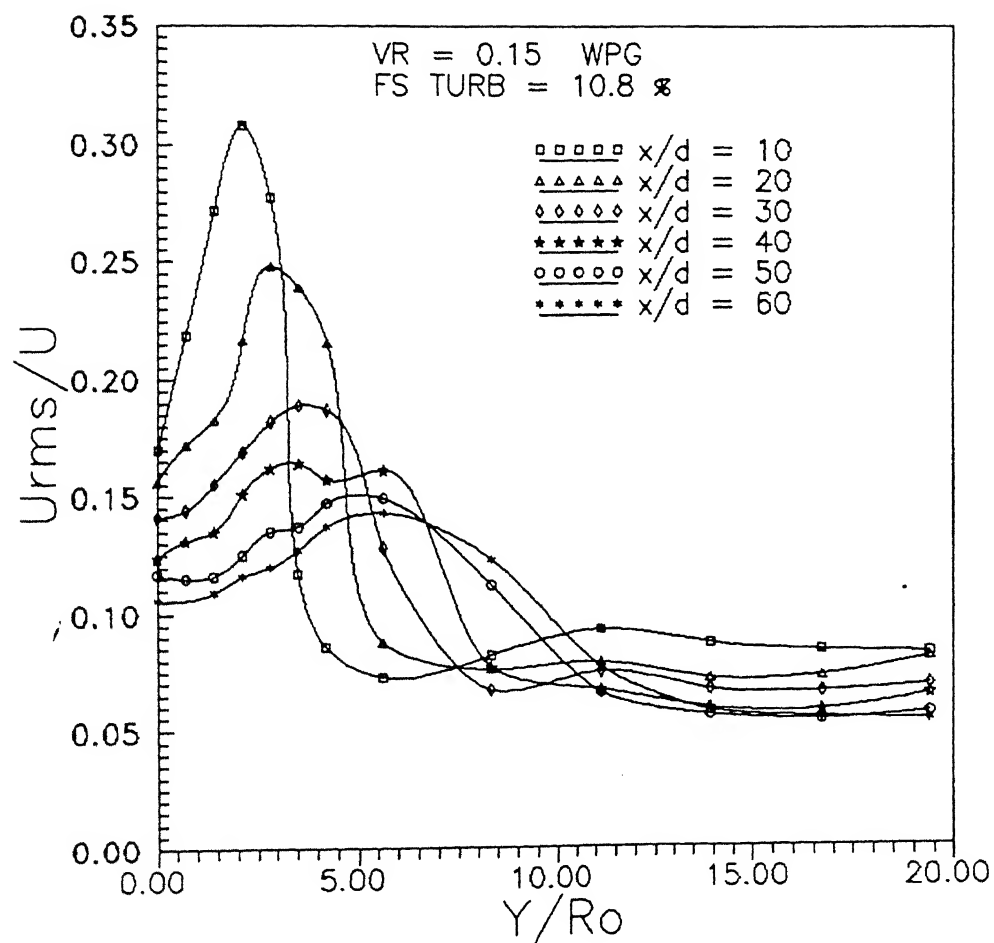


FIG.24. STREAMWISE TURBULENCE INTENSITY ACROSS THE FLOW

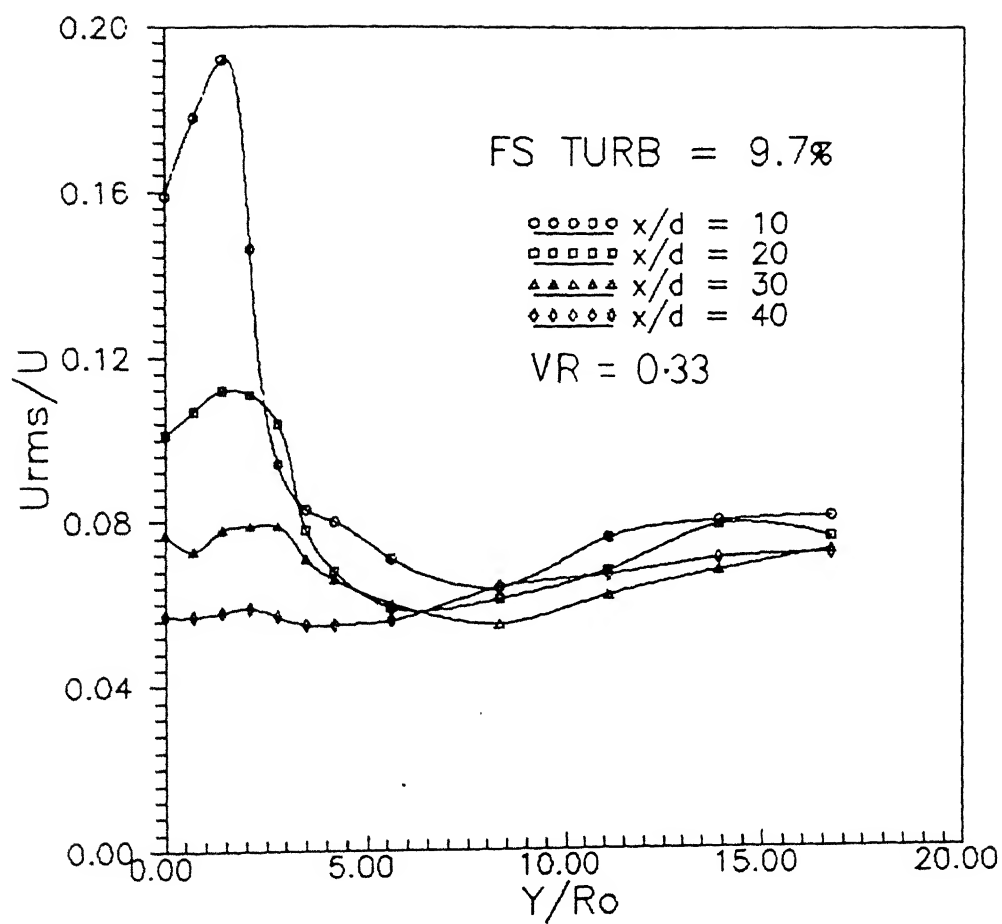


FIG.25 STREAMWISE TURBULENCE INTENSITY ACROSS THE FLOW

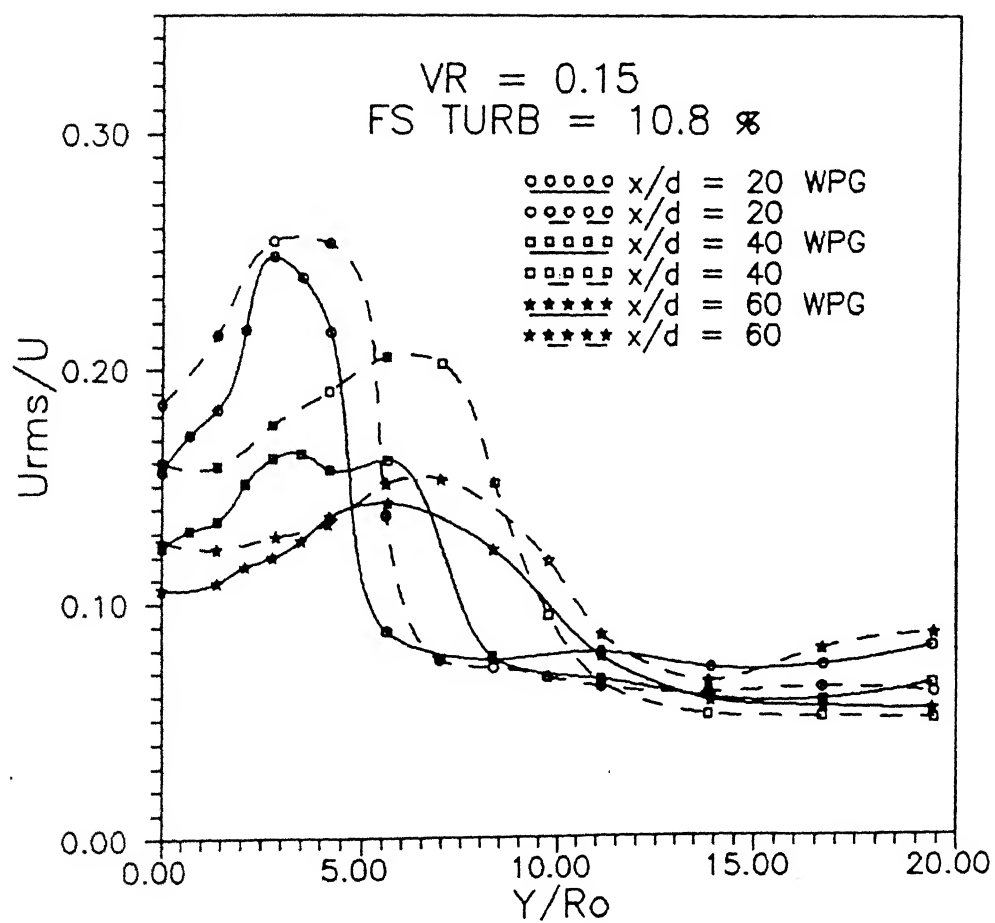


FIG.26. STREAMWISE TURBULENCE INTENSITY ACROSS THE FLOW

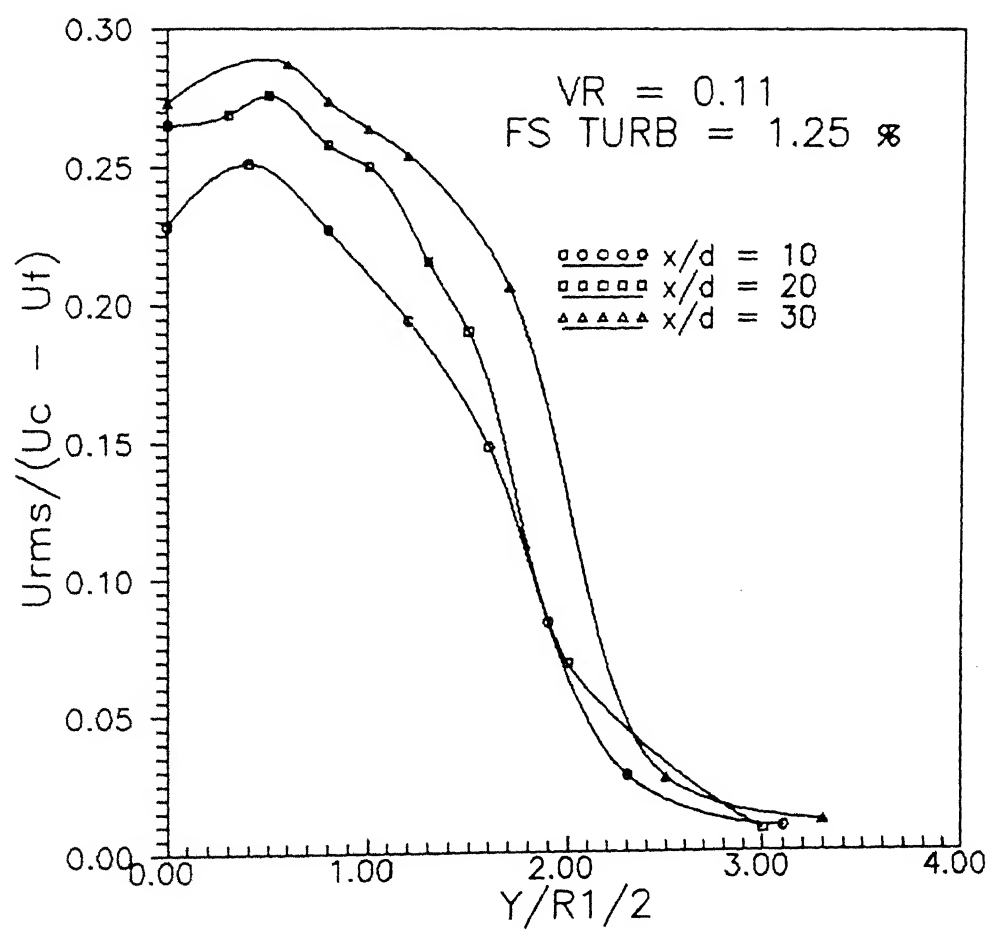


FIG.27 VARIATION OF U-INTENSITY ACROSS THE FLOW

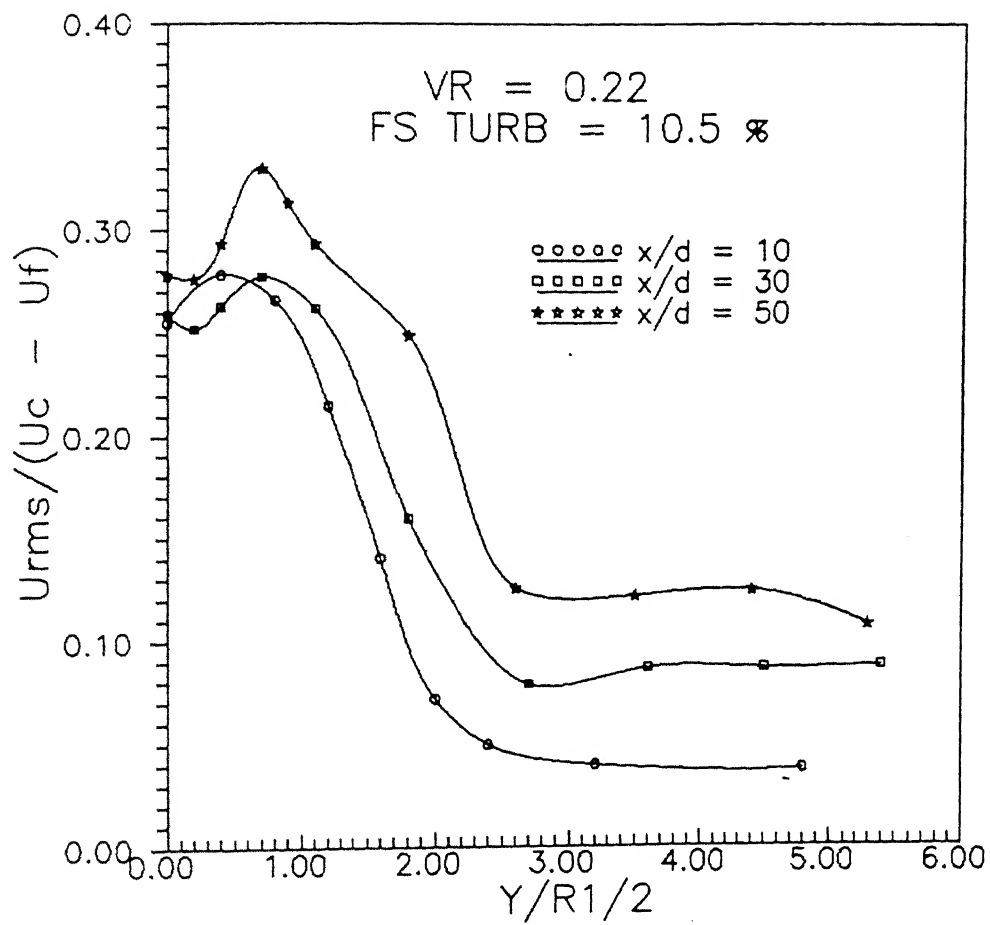


FIG.28 VARIATION OF U-INTENSITY ACROSS THE FLOW



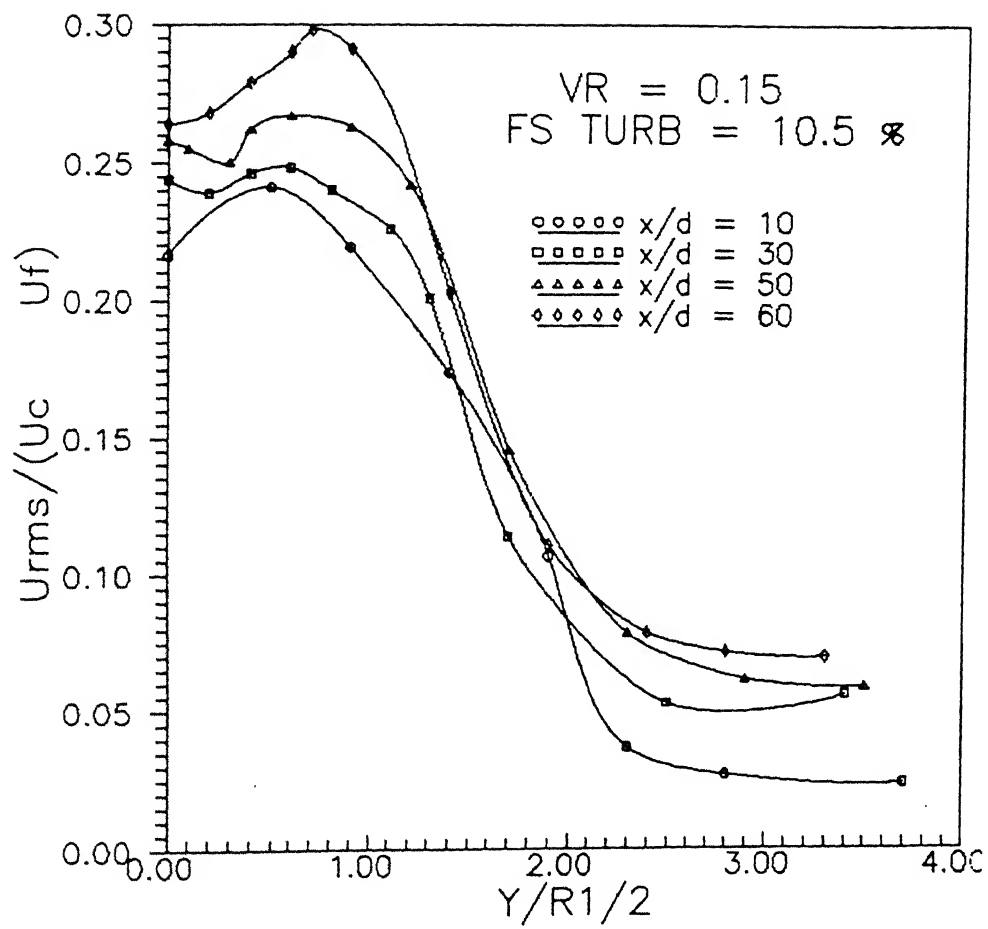


FIG.29 VARIATION OF U-INTENSITY ACROSS THE FLOW

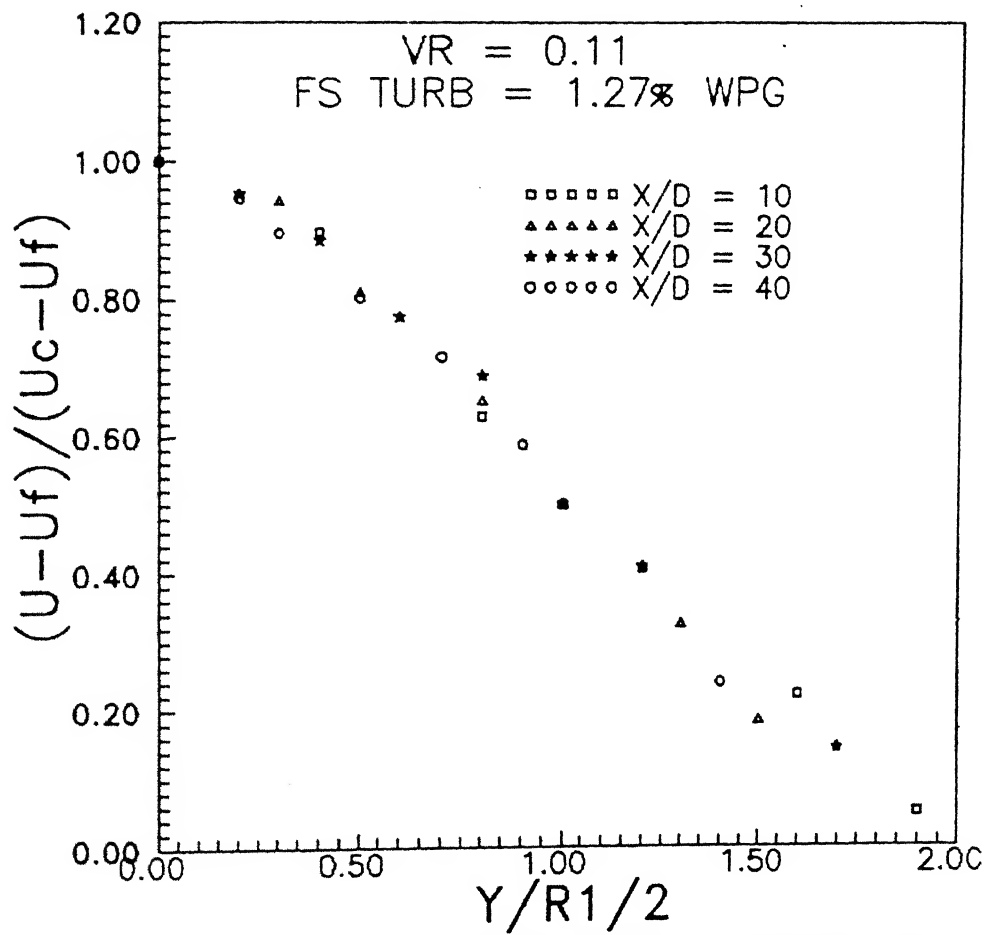


FIG 30. SIMILARITY OF VELOCITY PROFILES ACROSS THE FLOW

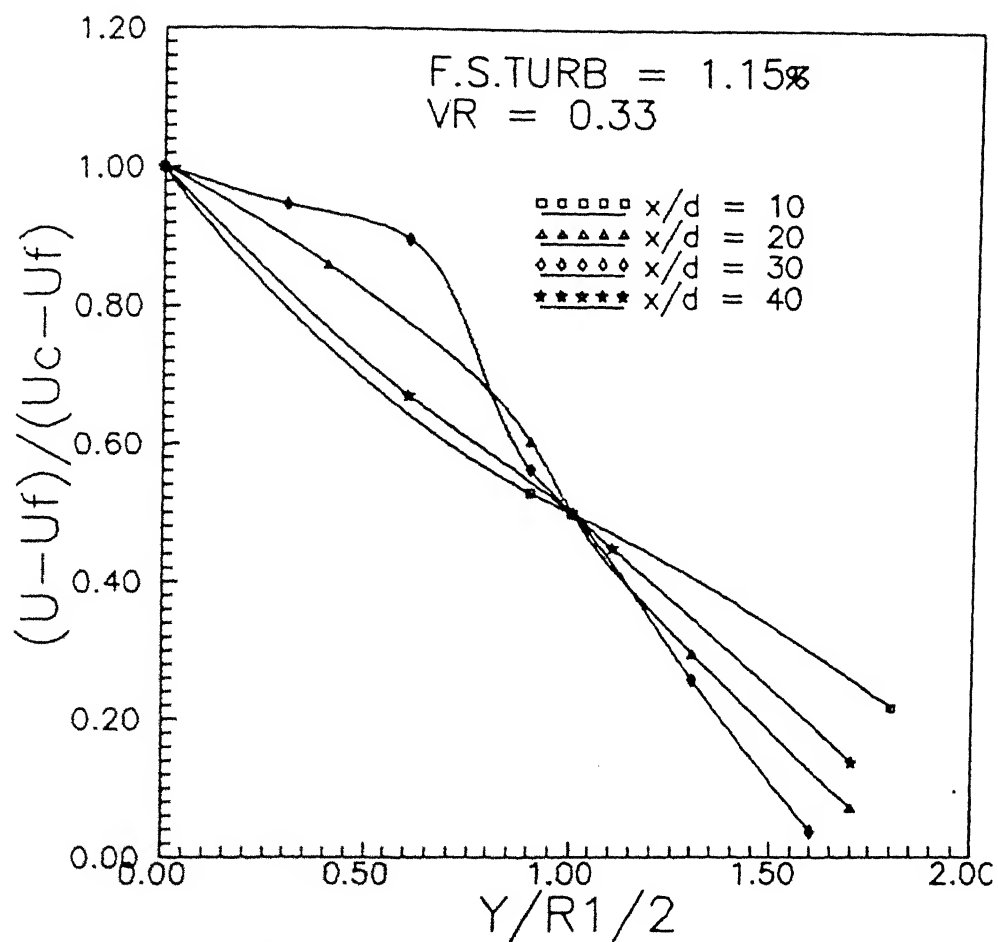


FIG.31 SIMILARITY OF VELOCITY PROFILE ACROSS THE FLOW

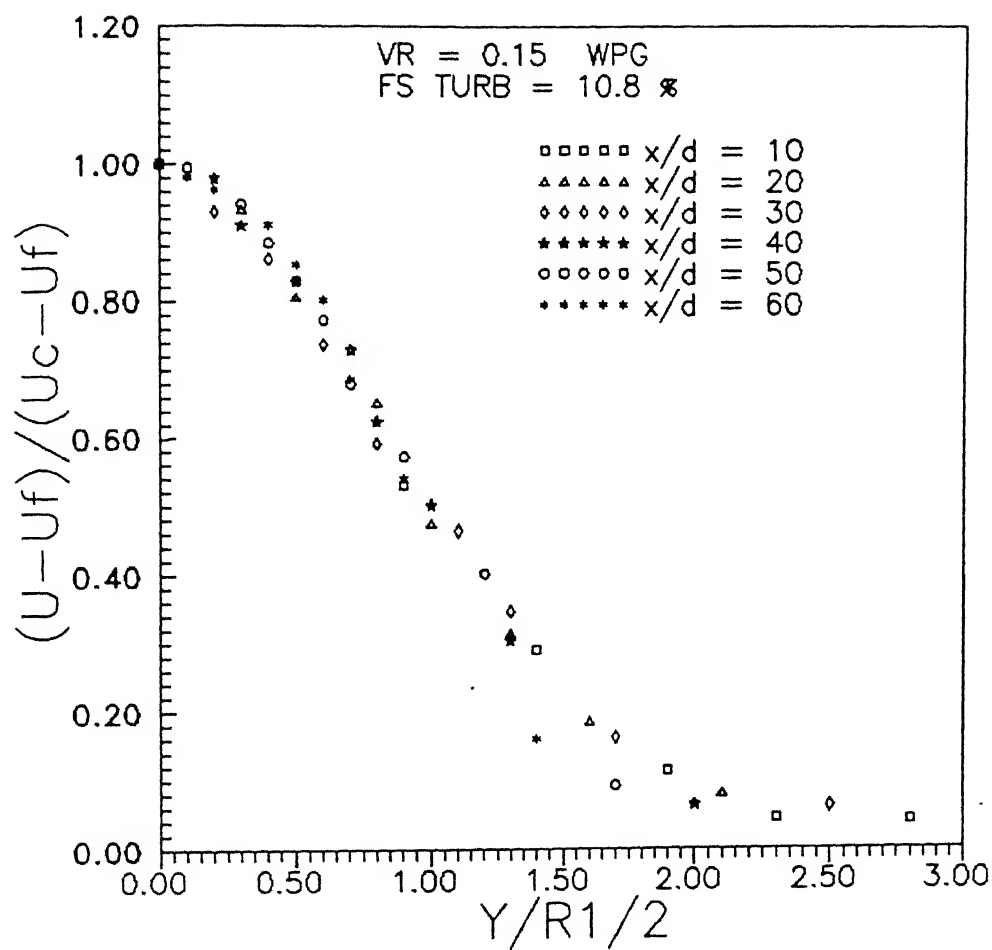


FIG.32. SIMILARITY OF VELOCITY PROFILES ACROSS THE FLOW

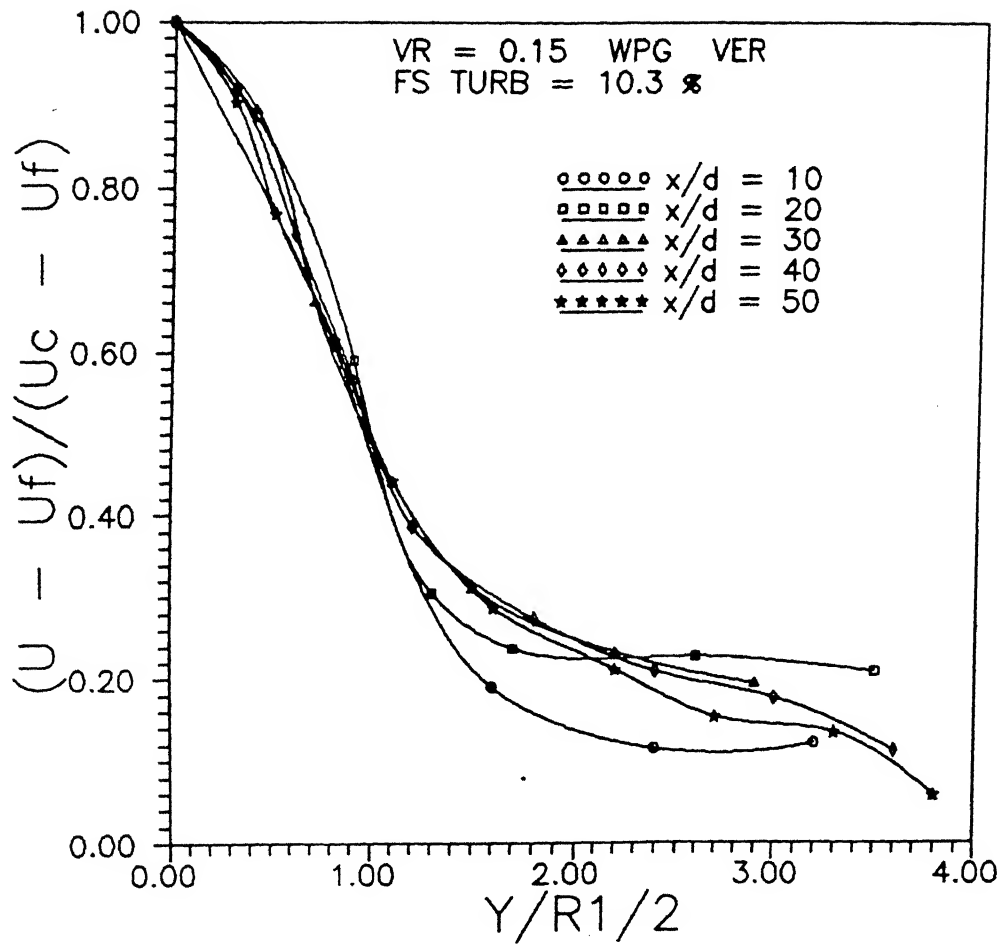


FIG.33. SIMILARITY OF VELOCITY PROFILES ACROSS THE FLOW

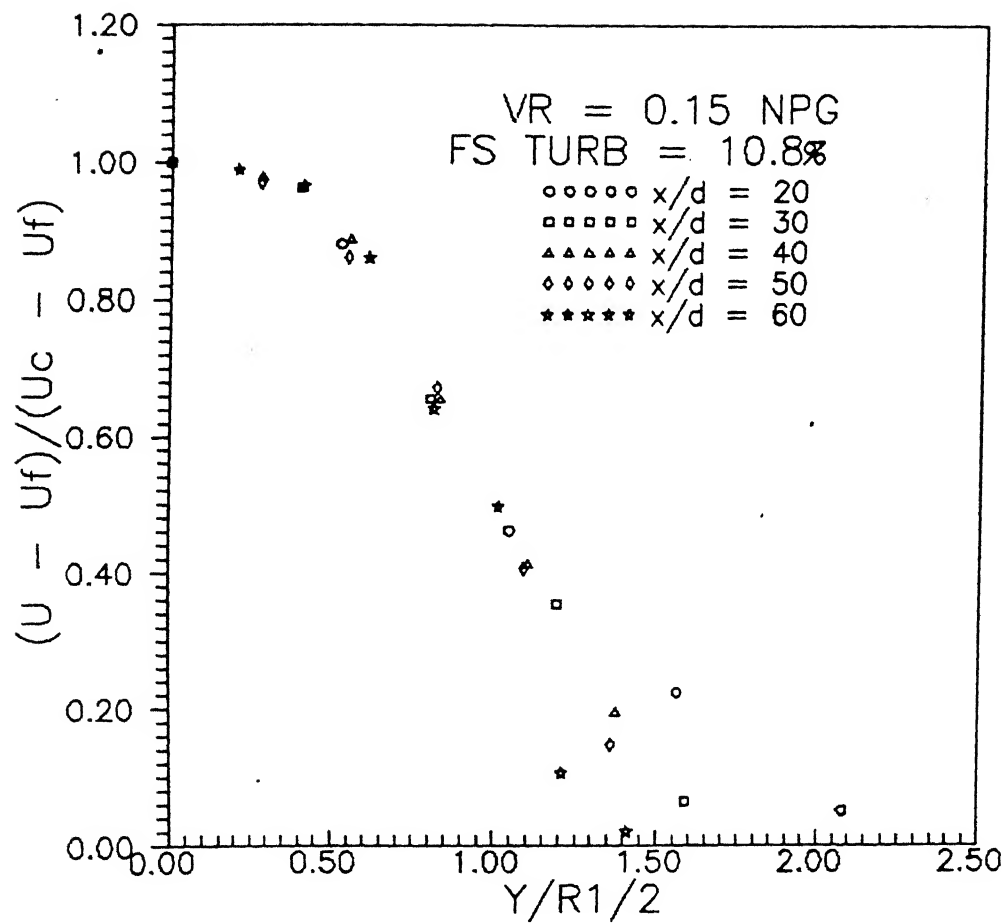


FIG.34 SIMILARITY OF VELOCITY PROFILES ACROSS THE FLOW